Slow-Light in Photonic Crystals Waveguides

by

Gisela López Galmiche

A Dissertation Submitted to the Program in Optics,
Optics Department

in Partial Fullfillment of the Requierements
for the Degree of

Master of Science in Optics

at the

National Institute for Astrophysics, Optics and Electronics

August 2012
Santa María Tonantzintla, Puebla

Advisors:

Prof. José Javier Sánchez Mondragón[1]
Prof. Ponciano Rodríguez Montero[1]
1 INAOE

Slow-light in Photonic Crystals Waveguides

Luz Lenta en Guías de Ondas de Cristales Fotónicos

Lic. Fis. Gisela Lopez Galmiche.

INAOE

Coordinación de Óptica

Tesis de Maestría en Ciencias

Especialidad en Óptica

Asesores:

Dr. José Javier Sánchez Mondragón

Dr. Ponciano Rodríguez Montero

Sta. María Tonantzintla, Pueb. México, agosto 2012.

Summary.

We modeled two realistic slow light structures, which are viable to be fabricated on silicon: Silicon strip waveguide photonic crystal with periodic SiO_2 holes and silicon *corrugated* waveguide. In order to modeling these devices we carried out simulations using the Plane Wave Expansion (PWE) method and the Finite Differences in Time Domain (FDTD) method. We employed the MIT Photonic Bands (MPB) free software developed by Massachusetts Institute of Technology and the FDTD Solutions software developed by Lumerical Solutions Inc.

Also, we analyzed the scattering originated by technological imperfections in the waveguides, known as extrinsic losses. In this analysis we used a theoretical model developed by T. Krauss group for described the losses effect in the photonic crystal waveguides. For this goal, a MPB code developed by the Krauss group was used.

Resumen.

En este trabajo se muestra el análisis de dos estructuras útiles para la propagación de luz lenta. El diseño de estas estructuras es realista y son viables para su fabricación en Silicio, ellas son: un alambre de silicio con agujeros periódicos de SiO_2 y una guía de onda con corrugaciones. Con la finalidad de modelar estos dispositivos, se llevó a cabo simulaciones empleando los métodos de expansión de onda plana (PWE) y de diferencias finitas en el dominio del tiempo (FDTD), para esto se utilizaron los programas MPB y FDTD Solutions, respectivamente.

Además, se analizó la dispersión originada por las imperfecciones tecnológicas en las guía de ondas, conocidas como las pérdidas extrínsecas. Para este análisis se utilizó un modelo teórico desarrollado por el grupo de T. Krauss, en el cual se describe el efecto de las pérdidas en las guías de cristal fotónico. Para este objetivo se utilizó el código MIT Photonic Bands (MPB).

Introduction.

A photonic crystal is part of a new breed of systems and tailored materials that have introduced recently to fully new realms on modern optics and photonics. They were initially designed in structures that were directly related to solid states physics and built up from materials readily available.

In particular, for a photonic crystal, it is essential to engineer the location and size of the bandgap and the crystal properties, which is done first by computational modeling and after experimentally confirmed. The design of the structured systems and photonic crystals involves the localization of specific periodic regions of high and low dielectric constants. The periodicity or spacing determines the relevant allowed or rejected light frequencies. One major advantage of photonics crystals is the possibility to design useful electromagnetic modes propagating through it. The ability to modify the bandgap dispersion allows precise control of the frequencies and directions of propagating electromagnetic waves. This feature makes them especially useful in optical telecommunications, laser sources, photonics chips, and so on. In general, such complicated structures are difficult to manufacture, even in the relatively controlled conditions of a laboratory.

However, for some particular parameters, Photonic wire Bragg structures are easy to fabricate using deep-UV photolithography. It is limited by light diffraction, which shrinks the minimum feature to a size about 50 nm. E-beam lithography shows higher resolution (20 nm), it is not diffraction-limited and allows versatile patterns fabrication.

Slow light is an interesting phenomenon characterized by low group velocities v_g in a medium, more specifically $v_g << c$. It has been applied in a vast span of applications such as optical delay lines or buffer, spectroscopy and to provide an efficient interaction in non-linear materials. It can be obtained in structured systems such as photonic crystals or Photonic wire grating structures. Sharp dispersion bands can exhibit flat regions in the dispersion curve where low v_g can be achieved. Such behavior can also be observed in W_1

PhC waveguides (waveguide with a linear defect) and strip waveguides with holes.

There are two types of losses in this structures: Intrinsic losses, such as diffraction losses by leaky modes; and extrinsic losses such as random variation of fabrication (disorder & surface roughness). However, scattering losses, which can be extrinsic and intrinsic, have done difficult the tailoring of all slow-light structures. Therefore, a great number of experiments are focusing in extrinsic and intrinsic losses nowadays. The design of the nanostructure geometry is idealized, but in the real world, imperfections in the geometry are frequently caused by fabrication process, meaning significant losses. In this work we analyze scattering losses, originated by technological imperfections in our waveguides. In particular, we analyze extrinsic losses. They are divided in backscattering losses and out of plane radiation losses that scale as n_g^2 and n_g, respectively.

Backscattering losses is a problem for any waveguide geometry. It has been observed and expected that they scales as n_g^2. This scaling factor is a serious limitation in the slow light regimen, such as Photonic crystals (PCs) with short propagation length. For this reason, a rich understanding of extrinsic losses is necessary.

As first step, the dispersion curves of the two slow-light structures proposed (corrugated waveguide and strip waveguide with SiO_2 holes) were modeled. We carried out the numerical analysis by utilizing the plane wave expansion (PWE) by using the MIT Photonic Bands (MPB) software. In the dispersion diagram, a band which slope is near to zero implies values of v_g that tend to zero, therefore for designing slow light structures we wish to model bands with a flat dependance. Our goal is to design and model PCS that shows a TE slow mono-mode solution near $\lambda \approx 1550$ nm with low losses. For these reason, we manipulate the geometrical parameters and find the dispersion curve for each device.

After that, we use the Finite Differences in Time Domain (FDTD) method to analyze the transmission spectrum for each device. We used the commercial

software “FDTD Solutions.” This method uses the time dependent Maxwell’s curl equations, where the derivatives in time are replaced by finite differences. Finally, we calculate those extrinsic losses using the Thomas Krauss MPB code whose results are further analyzed using a MATLAB routine.

In this work we designed and modeled two slow light devices: corrugated waveguide and strip waveguide with holes, which geometrical parameters can be fabricated using e-beam or UV photolithography techniques. Also, we carried out a loss analysis, more specifically losses caused by random fabrication variations, known as extrinsic losses. We got a value estimate of the success that the fabricated design fulfills the proposed design requirements, in the slow light regimen, strip waveguide with holes shows a value of group index $n_g = 8.5$ in a bandwidth of 14 nm which values of extrinsic losses of 1.3 dB/cm over the first Brillouin zone. While corrugated waveguide possess a $n_g = 7.8$ with extrinsic losses of 0.015 dB/cm over first Brillouin zone.

Acknowledgements.

This research project would not have been possible without the support of many people. I wish to express my gratitude to my supervisors PhD. Ponciano Rodríguez Montero who were abundantly helpful and offered invaluable assistance, support and guidance and PhD. J. Javier Sánchez Mondragón whose knowledge and assistance helped bring this work up.

I wish to express my sincere gratitude to Prof. Robert W. Boyd, Canada Excellence Research Chair in Quantum Nonlinear Optics, for providing me an opportunity to do my project. This project bears on imprint of many peoples. I sincerely thank to my project guides PhD. Sangeeta Murugkar and PhD. Israel De León, Department of Physics of University of Ottawa for their guidance and encouragement in carrying out this work.

Thanks to the CONACyT for providing the financial support. I also thank to the University of Ottawa for providing training and laboratory facilities in which this work was born; and to INAOE for providing me the opportunity to realize this graduate study.

Special thanks also to all my friends for sharing the literature and invaluable assistance. I wish to express my love and gratitude to my beloved families, in specially to my mother and my father; for their understanding and endless love throughout my studies.

PhD. Daniel Alberto May Arrioja
Proyecto: Desarrollo de Dispositivos Optofluidicos:
Integrados y en Fibra Óptica.
CONACyT CB-2010-01.
Clave Proyecto 157866.
PhD José Javier Sánchez Mondragón
Acoplamiento De Plasmones Y Ondas Nolineales (Solitones Espaciales y Ondas Superficiales).
CONACyT CB-2008.
Clave proyecto 101378.

Contents.

List of figures.

Chapter 1.- Photonic crystals.

1.1.- Introduction.

The aim of this chapter is the description of the slow-light devices proposed in this research project. In order to describe, the propagation of guided modes in photonic crystals we introduce the solution of the Maxwell's equations in terms of plane wave expansion (PWE) and finite differences by the time domain (FDTD) methods. We analyze the band structures, the supported modes and their propagation.

1.2.- Photonic crystals.

In 1987, Yablonovitch *(Eli Yablonovitch, 1987)* and John *(Sajeev John, 1987)* described periodic dielectric structures known as photonic crystals (PCs), which principal characteristic is a periodic refraction index of the order of the wavelength *(R. H. Lipson, 2009)*. Thomas Krauss made the first demonstration of a two-dimensional photonic crystal at optical wavelengths, *(Thomas F. Krauss R. M., 1996)*.

The one dimensional structural array of a PCs consist of two or more materials, stacked alternately, with high contrast of dielectric constant. In other words a layer with high permittivity ε_1 sandwiched by layers with low permittivity ε_2, such as $\varepsilon_1 > \varepsilon_2$. The Lattice constant is the spatial period in the slab, commonly denoted by a. PCs are analogous structures to crystals in solid state, for this reason, usually it is possible associate them with a Bravais lattice and much more complex structures may be designed.

Photonic crystals are dielectric and/or metals structures stacked that can control light. They are classified by the dimension of periodicity in three categories: one dimensional (1D), two dimensional (2D) & three dimensional (3D), see Figure 1.1.

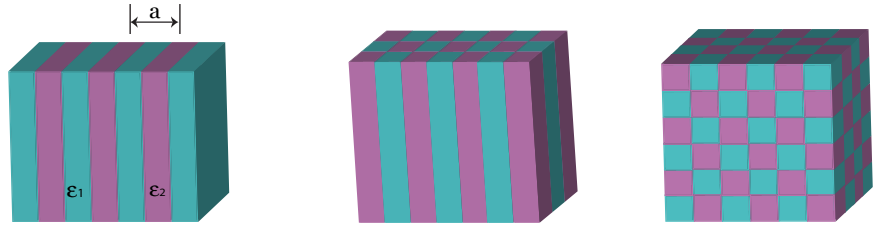

Figure 1.1.- Photonic crystals in 1D, 2D & 3D. Where "a" is the lattice constant, ε_1 y ε_2 are the dielectric constants of two materials with different refractive index stacked alternately and a as lattice constant.

In the same way that solid state, PCs show dispersion relations where the behavior of light is described by photonic bands. A photonic band gap (PBG) is a region where light is forbidden to propagate at specific frequencies, see Figure 1.2. And if, for some frequency range, the propagation of electromagnetic waves of *any* polarization and from *any* source are forbidden to travel in *any* direction, it is said that the Photonic crystal (PC) has a complete photonic band gap *(John D. Joannopoulos, 2008)*.

In order to obtain a specific behavior from a band or from a complete photonic bandgap, we first carry out its modeling in terms of the features or parameters of the specific photonic crystals. Some of them are dimensionality, symmetry, refractive index contrast and others.

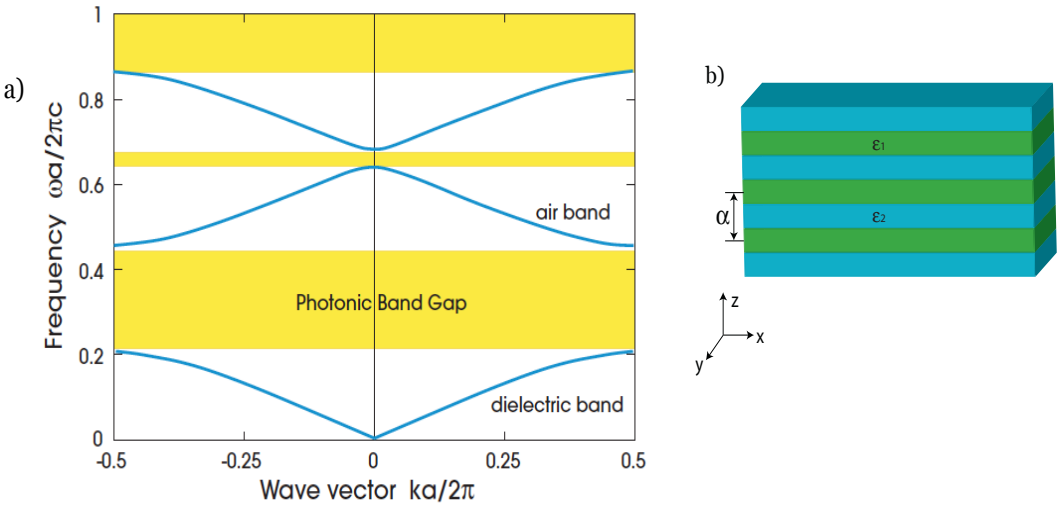

Figure 1.2.- a) The photonic band structure of a multilayer film. b) Multilayer film with lattice constant α, and alternating layers of different widths. The width of the ε_1=13 layer is 0.2 α, and the width of the ε_2=1 layer is 0.8 α. (John D. Joannopoulos, 2008).

A rich variety of physical phenomena have been demonstrated for these structures, which include super-prism, sub-wavelength imaging, focusing, collimation, and negative refraction with and without left-handed behavior *(Alessandro Massaro, 2012)*.

1.3.- Principle of index guiding.

Our first description of guiding is a ray like approach, and such approach is based in some of the most basic optical phenomenon. Reflection and refraction are familiar phenomena in optics. When an electromagnetic wave strikes the interface with an incidence angle θ_i respect to the normal, a part of the incident light is transmitted (or refracted) and other part is reflected. Snell´s law, given by Eq. (1.1), describes this phenomenon.

$$n_1 \sin\theta_i = n_2 \sin\theta_t \qquad (1.1)$$

Where n_1 and n_2 are the refractive index of the media respectively. θ_i and θ_t the incidence and transmitted angles.

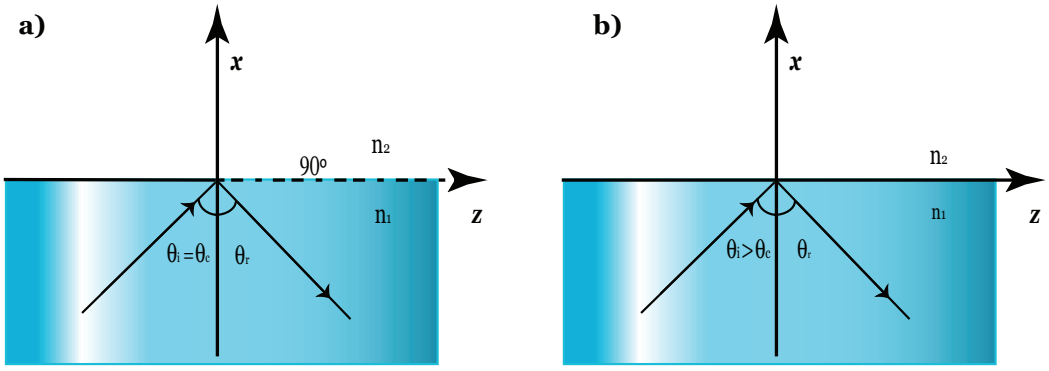

Figure 1.3.- TIR phenomenon. a) Critical angle $\theta_c = \theta_i$ for which all incident energy is reflected. b) All incident waves are reflected for angles $\theta_i \geq \theta_c$, no refracted waves appears.

Now, let is consider the propagation of light from the medium with refractive index n_1 to medium with n_2. We will assume that these media are homogeneous, isotropic and lossless. If it is assumed that $n_1 > n_2$ then it follows that $\theta_t > \theta_i$. From the Snell´s law, it is observed that there is certain angle $\theta_i \triangleq \theta_c$ for which $\theta_t \to 90°$, then there is not transmitted beam. This angle θ_c is known as critique angle and is given by:

$$\sin\theta_c = \frac{n_2}{n_1}. \qquad (1.2)$$

When this condition is met all the incident energy will be reflected to the incident medium. Obviously all energy is reflected for all the angles $\theta_i \geq \theta_c$. This phenomenon is known as the Total Internal Reflection (TIR), see Figure 1.3. TIR occurs in the medium with higher refractive index only, *(Eugene Hecht, 1998)*.

Now, let is consider a slab waveguide or a planar waveguide. This is a structure that consists of three layers with different refractive index. The

three different mediums are named superstrate, guide and substrate, with refractive indexes: n_1 , n and n_2 respectively. The principle of the transmission light in a waveguide is the TIR. To achieve the confinement of light is necessary that the TIR phenomenon occurs in the interfaces superstrate-guide and guide-substrate. Assuming that $n > n_1 > n_2$, this imply two critical angles, θ_{c1} and θ_{c2} .

$$\sin\theta_{c1} = \frac{n}{n_1} \tag{1.3}$$

$$\sin\theta_{c2} = \frac{n_2}{n} \tag{1.4}$$

There are three cases respect to propagation of light.

- The first case, *Air modes*, occurs for $n_1 = 1$(air) and the following angles $\theta_{c1} < \theta$ and $\theta_{c2} < \theta$. Light is propagated in radiation modes from substrate to superstrate. The confinement of light is no possible, because TIR is not satisfied in the two interfaces, Figure 1.4 (a).

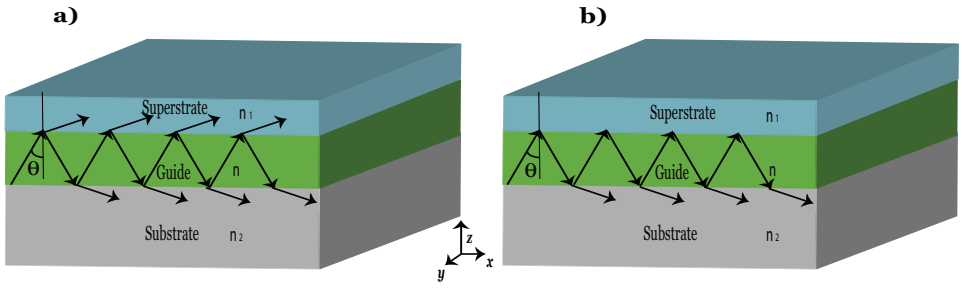

Figure 1.4.- Leaky modes are conformed by (a) Air modes and (b) Substrate modes. These phenomena are present in the waveguide when two or one interfaces do not satisfy the TIR.

- In the second case, known as *Substrate modes*, for $n_1 = 1$(air) and the angles $\theta_{c1} > \theta$ and $\theta_{c2} < \theta$. There are refractions in the interface guide-substrate and the TIR condition only happens in the interface guide-superstrate.

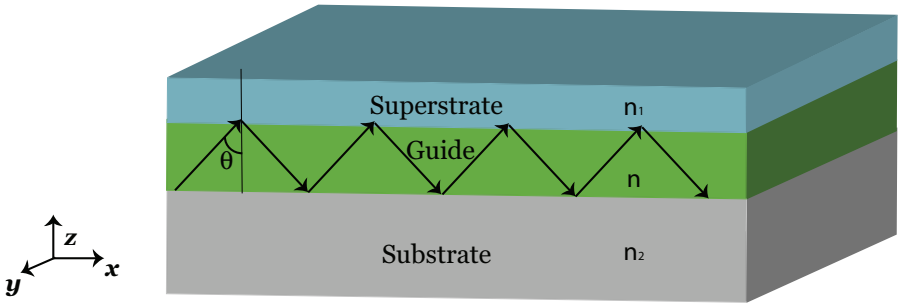

Figure 1.5.-Guides modes. A full confinement of light occurs.

Air and substrate modes conform the leaky modes. When light propagates in *x* direction, it can also propagates in *z* direction. This means that light can also manifest in leaky waves transversally the propagation direction. Actually, leaky modes have been used in the study of low losses in waveguides, (M. Miyagi, 1980).

- Finally, in the third case, Guided modes, for angles $\theta_{c1} > \theta$ and $\theta_{c2} > \theta$. The light is confined between the two interfaces: superstrate-guide and substrate guide*, (Azzedine Boudrioua, 2009)*. Because of the TIR, at both interfaces, the incident light is very well confined in the waveguide, while the transverse fields exponentially decay at the substrate and the superstrate media. Waveguides, optical fibers and others structures, use this principle to confine and transport light fields.

1.4.- Guided modes: Ray description.

A waveguide is a structure formed by a core and a cladding, with refractive index n_1 and n_2 respectively. The cladding has smaller refractive index than that the core $n_2 < n_1$. The surrounding environment is considers as well with a refractive index n_0; see Figure 1.6. The optical wave impinges the front face of the waveguide. Light enters into the core, where its confinement is given by the mechanism of Total Internal Reflection, *(Mohamad Azadeh, 2009)*.

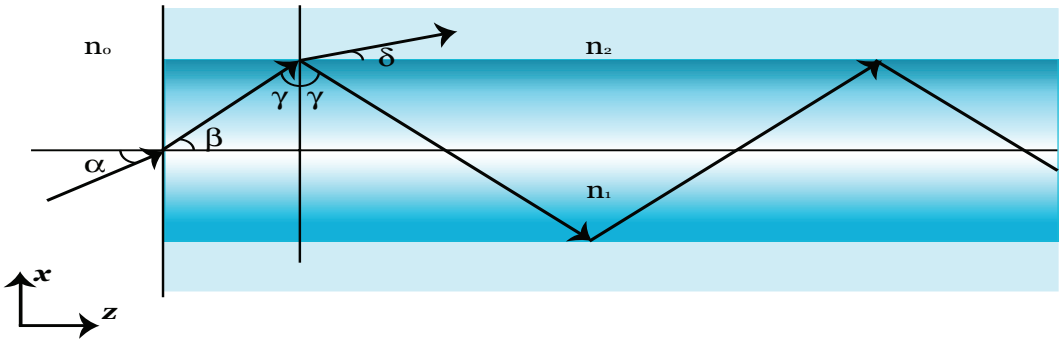

Figure 1.6.- Scheme using for the calculation of TIR in a waveguide.

The relation between of the refractive indexes: core, cladding and the surrounding environment is:

$$n_1 > n_2 \geq n_0 . \tag{1.5}$$

Using the Snell´s law in the interface surrounding environment-core.

$$n_0 \sin\alpha = n_1 \sin\beta \tag{1.6}$$

Applying again the Snell´s law in the interface core-cladding, it is getting the follow relation:

$$n_1 \sin\gamma = n_2 \sin\delta . \tag{1.7}$$

From the Figure 1.6, we realize that the angles β and γ are related by $\beta+\gamma=\pi/2$, then from the geometry of the problem $\sin\beta=\cos\gamma$. Therefore:

$$\sin\beta=\sqrt{1-\sin^2\gamma}. \tag{1.8}$$

The condition for TIR in the Eq. (1.7) is $\delta=\pi/2\Rightarrow\sin\delta=1$. Then,

$$\sin\gamma_{\max}=\frac{n_2}{n_1}. \tag{1.9}$$

By substituting Eq. (1.9) in Eq. (1.8), we obtain:

$$\sin\beta=\sqrt{1-\left(\frac{n_2}{n_1}\right)^2} \tag{1.10}$$

$$n_1\sin\beta=\sqrt{n_1^2-n_2^2}. \tag{1.11}$$

If we assume that the surrounding environment is air, $n_0=1$, and replacing the last equation in Eq. (1.6), then is obtain:

$$\sin\alpha=\sqrt{n_1^2-n_2^2} \tag{1.12}$$

$$\alpha_{\max}=\sin^{-1}\sqrt{n_1^2-n_2^2}. \tag{1.13}$$

The numerical aperture (NA) is defined as:

$$\sqrt{n_1^2-n_2^2}. \tag{1.14}$$

$\alpha_{\max}$ gives the maximum light angle in which the waves will be guided in the structure. The NA is a measure of difference of refractive index between core and cladding.

A waveguide can propagate a finite numbers of modes, which is related with a finite numbers of incidence angle, described by α_{max}. Then we can see that the refraction index contrast determines the propagated modes.

However, the ray theory cannot describe fully this phenomenon, for this reason it is necessary use the wave theory and therefore utilize the electromagnetics theory.

1.5.- Maxwell equations.

The Electromagnetic field behavior in a photonic crystal is described by the Maxwell equations.

$$\nabla \cdot \vec{B}(\vec{r},t) = 0 \tag{1.15}$$

$$\nabla \cdot \vec{D}(\vec{r},t) = \rho \tag{1.16}$$

$$\nabla \times \vec{E}(\vec{r},t) + \frac{\partial \vec{B}(\vec{r},t)}{\partial t} = 0 \tag{1.17}$$

$$\nabla \times \vec{H}(\vec{r},t) - \frac{\partial \vec{D}(\vec{r},t)}{\partial t} = \vec{J}(\vec{r},t) \tag{1.18}$$

Now, the propagation of light in a mixed dielectric medium is analyzed, see Figure 1.1, 3D. It possesses homogeneous regions of dielectric material, where there are not free charges neither currents, that is imply $\rho = 0$ and $\vec{J}(\vec{r},t) = 0$. In order to simplify the analysis the following assumptions are made:

- The material is isotropic, this means that $\vec{E}(\vec{r},t)$ and $\vec{D}(\vec{r},t)$ can be related by a constant $\varepsilon(\vec{r},\omega)\cdot\varepsilon_0$, where $\varepsilon(\vec{r},\omega)$ is the dielectric constant function and ε_0 as dielectric constant for free space.

- This dielectric constant function perfectly periodic with respect to spatial position vector $\vec{r}$, isotropic and independent on the light frequency.
- For small field strengths, the electric susceptibility χ and $\varepsilon(\vec{r},\omega)$ do not dependent on electric field $\vec{E}(\vec{r},t)$. Therefore, the nonlinear effects can be ignored.
- The dielectric function $\varepsilon(\vec{r})$ must be taken as real, transparent medium.
- Because the material is not polarizable, the electric susceptibility χ of material can be neglected.
- The relative magnetic permeability $\mu(\vec{r})$ of the material is taken as the unity.

Under the previous assumptions, displacement field $\vec{D}(\vec{r},t)$ and the magnetic induction $\vec{B}(\vec{r},t)$ are given by:

$$\vec{D}(\vec{r},t)=\varepsilon_0\varepsilon(\vec{r})\vec{E}(\vec{r},t) \tag{1.19}$$

$$\vec{B}(\vec{r},t)=\mu_0\vec{H}(\vec{r},t). \tag{1.20}$$

Now, when they are substituted Eq. (1.20) and Eq. (1.19) into of the equations set from Eq. (1.15) to Eq. (1.18), it is obtained:

$$\nabla\cdot\vec{H}(\vec{r},t)=0 \tag{1.21}$$

$$\nabla\cdot\left[\varepsilon(\vec{r})\vec{E}(\vec{r},t)\right]=0 \tag{1.22}$$

$$\nabla\times\vec{E}(\vec{r},t)+\mu_0\frac{\partial\vec{H}(\vec{r},t)}{\partial t}=0 \tag{1.23}$$

$$\nabla\times\vec{H}(\vec{r},t)-\varepsilon_0\varepsilon(\vec{r})\frac{\partial\vec{E}(\vec{r},t)}{\partial t}=0. \tag{1.24}$$

By using the linearity property of Maxwell equations, it is possible to separate the fields in a time sinusoidal expression and an expression dependent on the spatial coordinates:

$$\vec{H}(\vec{r},t) = \vec{H}(\vec{r})E\,\mathrm{xp}[-i\omega t] \tag{1.25}$$

$$\vec{E}(\vec{r},t) = \vec{E}(\vec{r})Exp[-i\omega t]. \tag{1.26}$$

By substituting Eq. (1.25) and Eq. (1.26) into the equations set Eq. (1.21)-Eq. (1.24), it is generated:

$$\nabla \cdot \vec{H}(\vec{r}) = 0 \tag{1.27}$$

$$\nabla \cdot \left[\varepsilon(\vec{r})\vec{E}(\vec{r})\right] = 0 \tag{1.28}$$

$$\nabla \times \vec{E}(\vec{r}) - i\omega\mu_0 \vec{H}(\vec{r}) = 0 \tag{1.29}$$

$$\nabla \times \vec{H}(\vec{r}) + i\omega\varepsilon_0 \varepsilon(\vec{r})\vec{E}(\vec{r}) = 0. \tag{1.30}$$

Which are known as the spatial-dependent Maxwell equations. The first two equations imply that there are not sinks or sources of $\vec{E}(\vec{r})$ and $\vec{D}(\vec{r})$ in the medium. The set of Maxwell equations in which the curl is involved are decoupled dividing by $\varepsilon(\vec{r})$ and taking the curl to Eq. (1.30).

$$\nabla \times \left[\frac{1}{\varepsilon(\vec{r})}\nabla \times \vec{H}(\vec{r})\right] = \left(\frac{\omega}{c}\right)^2 \vec{H}(\vec{r}) \tag{1.31}$$

Where the light velocity in the vacuum is given by $c = \frac{1}{\sqrt{\varepsilon_0\mu_0}}$. In a similar way for Eq. (1.29):

$$\frac{1}{\varepsilon(\vec{r})}\nabla \times \left[\nabla \times \vec{E}(\vec{r})\right] = \left(\frac{\omega}{c}\right)^2 \vec{E}(\vec{r}) \tag{1.32}$$

$$\nabla \times \left[\nabla \times \frac{1}{\varepsilon(\vec{r})}\vec{D}(\vec{r})\right] = \left(\frac{\omega}{c}\right)^2 \vec{D}(\vec{r}). \tag{1.33}$$

The equations Eq. (1.31) and Eq. (1.32) are called as master equations; they

bring all necessary information about fields. The macroscopic field $\vec{E}(\vec{r})$ is not a continuum function from Eq. (1.31) throughout their magnetic field components, while the field $\vec{H}(\vec{r})$ the operator applied to the left side of Eq. (1.31) is Hermitian and $\vec{H}(\vec{r})$ is continuous throughout their magnetic field components, *(J. D. Joannopoulos, 1995)*. For a refractive index distribution and a given frequency, the Eq. (1.31) has possible algebraic solutions. However, Eq. (1.32) cannot be resolve as a simple problem.

They are formulated as an eigenvalue problem, so for solving them, it is necessary to employ numerical methods, such as plane wave expansion or finite time difference, *(K. Busch, 2002)*.

1.6.- Guided modes: Wave description.

In order to produce a wave equation for the electromagnetic field from the Maxwell´s equations, we take the curl in the Eq. (1.23) and considering the vector identity:

$$\nabla \times \nabla \times \vec{A} = \nabla(\nabla \cdot \vec{A}) - \nabla^2 \vec{A} \tag{1.34}$$

The following expression is obtained:

$$\nabla^2 \vec{E}(\vec{r},t) = \mu_0 \frac{\partial}{\partial t} \nabla \times \vec{H}(\vec{r},t). \tag{1.35}$$

Then, taking Eq. (1.24) and combined with Eq. (1.35), the wave equation for electric field, $\vec{E}(\vec{r},t)$ is obtained:

$$\nabla^2 \vec{E}(\vec{r},t) = \mu_0 \varepsilon_0 \varepsilon(\vec{r}) \frac{\partial^2 \vec{E}(\vec{r},t)}{\partial t^2}. \tag{1.36}$$

From a similar way, the wave equation for magnetic field is:

$$\nabla^2 \vec{H}(\vec{r},t) = \mu_0 \varepsilon_0 \varepsilon(\vec{r}) \frac{\partial^2 \vec{H}(\vec{r},t)}{\partial t^2}. \qquad (1.37)$$

The solution of this wave equation provides us the information with the information on the behavior of light in the waveguide. Discrete solutions are a consequence of the application of the boundary conditions, also known as modes. The dimensions of the structure select the propagated modes in the waveguide. Because the size of the waveguide is finite, it can only support a finite number of modes, *(Mohamad Azadeh, 2009)*.

The waves propagate in *z* direction because in this axis there are no reflections, while the propagation in *x* direction is avoid by the TIR condition, see Figure 1.6. Nevertheless, the waves are reflected back to core in the core-cladding boundary over *x* direction.

The fundamental mode has a peak in the center of the waveguide and, in the boundary their power profile does not go to zero abruptly. Evanescent fields, with exponentially decaying profile in *x* direction, are propagated together the fundamental mode in the *z* direction, *(Mohamad Azadeh, 2009)*.

1.7.- Bloch Theorem.

The characteristic of a Photonic Crystal is it material periodicity, therefore it is important to know the Bloch theorem, that deals precisely with this kind of problems. It states that:

"The eigen functions of the wave equation for a periodic potential are the product of a plane wave $Exp\left[i(\vec{k}\cdot\vec{r})\right]$ *times a function* $\vec{u}_{\vec{k}}(\vec{r})$ *with the periodicity of the crystal lattice". (Charles Kittel, 1996).*

$$\vec{\psi}_{\vec{k}}(\vec{r}) = \vec{u}_{\vec{k}}(\vec{r})Exp\left[i(\vec{k}\cdot\vec{r})\right] \tag{1.38}$$

Where the function $\vec{u}_{\vec{k}}(\vec{r})$ has the period lattice of the crystal, with the following property:

$$\vec{u}_{\vec{k}}(\vec{r}) = \vec{u}_{\vec{k}}(\vec{r}+\vec{R}). \tag{1.39}$$

Felix Bloch gave the solutions for an eigen problem whose potential posses translational symmetry.

The Bloch function $\vec{u}_{\vec{k}}(\vec{r})$ has the same periodicity that the potential. This theorem can be applied in problems with periodic media, such as photonic crystals.

1.8.- Wave plane expansion.

One method to determinate the bandgaps in photonic crystals is the plane wave expansion. This takes advantage of the periodicity lattice by expanding the fields in terms of Bloch vectors. Then, the eigen formulation of the Maxwell's equations is used for calculating the band structure, and thus solving for eigen frequencies for each propagation directions of the wave vector, *(Alessandro Massaro, 2012)*.

The macroscopic field $\vec{D}(\vec{r})$ and its master equation Eq. (1.33) could be used for solving the problem, but the operator applied to left side of $\vec{D}(\vec{r})$ is not Hermitian in Eq. (1.33). In the case of the field $\vec{E}(\vec{r})$, this is not a continuous function, *(Mikhail A. Noginov G. D., 2009)*. However, for the field $\vec{H}(\vec{r})$ the operator applied to the left side of Eq. (1.31) is Hermitian and $\vec{H}(\vec{r})$ is continuous throughout their magnetic field components, *(J. D. Joannopoulos, 1995)*. A Hermitian operator works the same way to the right or to the left under products of the integral, see expression Eq. (1.40). This involves a complete set of eigen functions which eigen values are real.

$$\int \vec{H}^* \cdot \left[\nabla \times \frac{1}{\varepsilon(\vec{r})} \nabla \times \vec{H} \right] = \int \left[\nabla \times \frac{1}{\varepsilon(\vec{r})} \nabla \times \vec{H} \right]^* \cdot \vec{H} \qquad (1.40)$$

That the operator be Hermitian and positive definite has as consequence real eigen frequencies ω. The squared frequencies of theses modes are proportional to their eigenvalues $\left(\frac{\omega}{c}\right)^2$.

In the reciprocal space (space in frequencies domain) the expressions for $\vec{H}(\vec{r})$ and $\vec{E}(\vec{r})$, *(Kazuaki Sadoka, 2001), (Mikhail A. Noginov G. D., 2009)* are:

$$\vec{H}(\vec{r}) = \sum_{\vec{G}} \vec{H}(\vec{G}) Exp\left[i(\vec{k} + \vec{G}) \cdot \vec{r} \right] \qquad (1.41)$$

$$\vec{E}(\vec{r}) = \sum_{\vec{G}} \vec{E}(\vec{G}) Exp\left[i(\vec{k} + \vec{G}) \cdot \vec{r} \right]. \tag{1.42}$$

Where $\vec{G} = a_1\vec{b}_1 + a_2\vec{b}_2 + a_3\vec{b}_3$ is a vector of the reciprocal lattice space and $\vec{k}$ as wave vector in real space (Brillouin zone). Because of the periodicity spatial of dielectric function $\varepsilon(\vec{r})$, it is possible expand in Fourier series the function $\varepsilon^{-1}(\vec{r})$.

$$\frac{1}{\varepsilon(\vec{r})} = \sum_{\vec{G}''} \varepsilon(\vec{G}'') Exp\left[i(\vec{G}'' \cdot \vec{r}) \right] \tag{1.43}$$

Substitution of Eq. (1.43) and Eq. (1.41) in Eq. (1.31), gives:

$$\nabla \times \left[\sum_{\vec{G}''} \varepsilon(\vec{G}'') Exp\left[i\left(\vec{G}'' \cdot \vec{r} \right) \right] \nabla \times \sum_{\vec{G}} \vec{H}(\vec{G}) Exp\left[i\left(\vec{k} + \vec{G} \right) \cdot \vec{r} \right] \right]$$
$$= \left(\frac{\omega}{c} \right)^2 \sum_{\vec{G}} \vec{H}(\vec{G}) Exp\left[i\left(\vec{k} + \vec{G} \right) \cdot \vec{r} \right] \tag{1.44}$$

Using $\vec{G} = \vec{G}' + \vec{G}''$ it can be rewritten as:

$$\nabla \times \left[\sum_{\vec{G}} \varepsilon\left(\vec{G} - \vec{G}' \right) Exp\left[i\left(\vec{G} - \vec{G}' \right) \cdot \vec{r} \right] \nabla \times \sum_{\vec{G}'} \vec{H}\left(\vec{G}' \right) Exp\left[i\left(\vec{k} + \vec{G}' \right) \cdot \vec{r} \right] \right]$$
$$= \left(\frac{\omega}{c} \right)^2 \sum_{\vec{G}} \vec{H}\left(\vec{G} \right) Exp\left[i\left(\vec{k} + \vec{G} \right) \cdot \vec{r} \right] \tag{1.45}$$

By using the following relations:

$$\nabla \times \left(\vec{V} Exp\left[i(\vec{u} \cdot \vec{r}) \right] \right) = i\vec{u} \times \vec{V} Exp\left[i(\vec{u} \cdot \vec{r}) \right] \tag{1.46}$$

$$\nabla \times \left(\left[\nabla \times \vec{V} Exp\left[i(\vec{u} \cdot \vec{r}) \right] \right] \right) = -\vec{u} \times \left[\vec{u} \times \vec{V} Exp\left[i(\vec{u} \cdot \vec{r}) \right] \right]. \tag{1.47}$$

Applying twice the first relation given by Eq. (1.46) to Eq. (1.45) and using the non-commutative property of the vectorial product one arrives to the equation:

$$-\sum_{\vec{G}} \sum_{\vec{G}'} \varepsilon(\vec{G} - \vec{G}')(\vec{k} + \vec{G}) \times \left[(\vec{k} + \vec{G}) \times \vec{H}(\vec{G}') \right] e^{i(\vec{k}+\vec{G})\cdot\vec{r}} = \left(\frac{\omega}{c} \right)^2 \sum_{\vec{G}} \vec{H}(\vec{G}) e^{i(\vec{k}+\vec{G})\cdot\vec{r}} \tag{1.48}$$

$$-\sum_{\vec{G}}\varepsilon\left(\vec{G}-\vec{G}'\right)\left(\vec{k}+\vec{G}\right)\times\left[\left(\vec{k}+\vec{G}\right)\times\vec{H}\left(\vec{G}'\right)\right]=\left(\frac{\omega}{c}\right)^2\sum_{\vec{G}}\vec{H}\left(\vec{G}\right). \quad (1.49)$$

Where it was taken the projection Eq. (1.48) onto the basis function $Exp\left[i\left(\vec{k}+\vec{G}\right)\cdot\vec{r}\right]$, *(Jean-Michel Lourtioz, 2005).*

With an analogous process for the field $\vec{E}(\vec{r})$ it can obtain the following expression for $\vec{E}\left(\vec{G}\right)$:

$$-\sum_{\vec{G}'}\varepsilon\left(\vec{G}-\vec{G}'\right)\left(\vec{k}+\vec{G}\right)\times\left[\left(\vec{k}+\vec{G}\right)\times\vec{E}\left(\vec{G}'\right)\right]=\left(\frac{\omega}{c}\right)^2\sum_{\vec{G}}\vec{E}\left(\vec{G}\right). \quad (1.50)$$

Expressions Eq. (1.49) and Eq. (1.50) are also known as the master equations. These eigen value equations were obtained by Fourier expansion coefficients of fields $\vec{H}(\vec{r})$ and $\vec{E}(\vec{r})$. Because the components of $\vec{E}(\vec{r})$ are not continuous (they are not tangential to the dielectric interface) and to the non-Hermitian operator in the left side of Eq. (1.32), the use of the master equation for $\vec{E}(\vec{r})$ is generally avoid.

PCs are complex vectorial systems to solve analytically, in special 3D systems. Plane wave expansion works in the reciprocal space, where utilizing the translational symmetry can be determinate the solutions. For this aim are taking the k vectors restricted to first Brillouin zone.

The Brillouin zone is described as a Wigner-Seitz primitive cell in the reciprocal space. The value of this zone provides a geometrical interpretation of the diffraction condition $2\vec{k}\cdot\vec{G}=\vec{G}^2$, where $\vec{G}$ is the reciprocal vector. This condition shows the wavevectors $\vec{k}$ that can be reflected by the crystal. The first Brillouin zone is the small volume entirely closed by planes that are perpendicular bisectors of the reciprocal lattice vectors drawn from the origin *(Charles Kittel, 1996)*.

Substituting the expansions given by Eq. (1.49) in the master equation Eq. (1.31) is obtain an infinite matrix eigen problem. After the matrix is suitably truncated, the solutions to the before mentioned problem provide the eigen frequencies and expansion coefficients for the eigen functions, *(S. Fan P. R., 1994)*.

The dispersion relations are constituted when a certain Bloch wave vector $\vec{k}$ posses a determined value allowed for a frequency ω. That is equivalent to diagonalization of the matrix localized in left side of Eq. (1.49) and Eq. (1.50). The numerical calculations must have a sufficiently large number N of reciprocal vector $\vec{G}'$. In other words N is the number of plane waves and the accuracy of the method increases with this parameter.

1.9.- Finite difference time domain.

Finite difference time domain (FDTD) method is a modeling technique it uses the time dependent Maxwell's curl equations, where the derivates in time are replaced by finite differences. Such method has been extensively used in a variety of electromagnetic problems as scattering, propagation and radiation.

Finite differences were first applied to Maxwell's curl equations in the work of Kane S. Yee in 1966, *(Kane S. Yee, 1966)*. Yee cell-method is a famous of discretization of Maxwell´s equations in FDTD. In particular, a Yee cell is a cubic unit cell with an orthogonal spatial grid, see Figure 1.7.

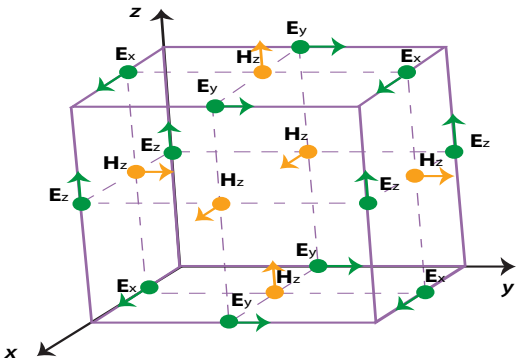

Figure 1.7.- A Yee cell is an unit cell where the electric and magnetic fields are distributed in their components around their spatial grid.

Starting from initial conditions, it is possible, in a specific region, to get the temporal evolution of electromagnetic fields in the following way: For a particular time, the magnetic/electric field is calculated over a grid point, depending of the values of electric/magnetic field of the adjacent nodes and the previous time instant. Each field vector component is related with a particular grid point, this implies a linear equation system. In discrete time-steps, where $\triangle t$ is the time-step, the fields components are updated at intervals of $\triangle t/2$.

The discretization of the time dimension depends of frequency, materials (region) and spatial discretization. Electrics and magnetic fields do not concur in time. There is a temporal entanglement between the fields, caused by the derivative of time evaluated in different and consecutive time instants.

The FDTD method can solve difficult problems in many areas as: microwaves, antennas, photonic crystals, plasmons, solitons and bio photonics. But a large computational domain must close the structure and its infinity extension is simulated by a suitable boundary condition on the outer perimeter of the domain. For this reason computational costs are expensive, because a large computational time and large amount of memory.

However, this method has been popularized because of its flexibly and its power to model electrodynamics problems. Some of its advantages are: it can modelate arbitrary symmetries, sources of different types can be easily modelated too and the programming is relatively easy, *(S. González García, 2004)*.

I have used available numerical software to model the proposed structures. The first one is the Massachusetts Institute of Technology Photonic Bands (MPB) software. This is a free software and it allows us to solve the master equations using the Plane Wave Expansion (PWE). The second numerical method Finite Differences in Time Domain (FDTD) Solutions is a commercial software. At the beginning of this project, I used one license at the University of Ottawa, where I made my research internship. In the final stage of the project I used a trial license (solutions).

1.10.- Periodic waveguides.

Nowadays, 1D Periodic waveguides are relatively easy to fabricate. These structures shows periodic pattern. Their main characteristic is that they can confine light in a different direction respect to the periodic direction; as consequence, they build up a photonic band gap in their periodic direction using the principle of Index guiding.

In this work the interesting subject will be the waveguides with one-dimensional periodic pattern along the propagation direction of the light only where width and thickness are finite. Some examples of such structures are schematized in Figure 1.8. These structures show the photonic band gaps along the periodic direction which light is propagated. In the case of Figure 1.8 (a), the photonic band gap is in x direction, while the confinement of light is given in y direction, *(John D. Joannopoulos, 2008)*. This periodicity condition implies a well-defined Bloch wavenumber k and, as consequence the light can travel into the structure without reflections.

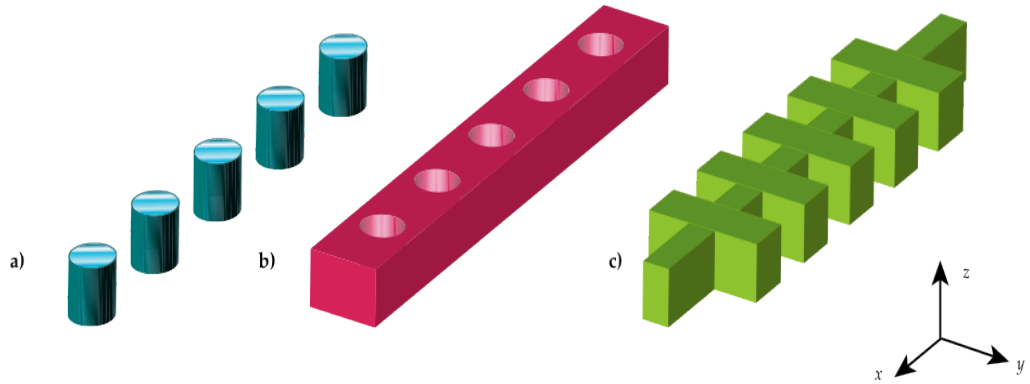

Figure 1.8.- Periodic waveguides with index guiding in two transversal directions.

A waveguide under reflections is symmetric respect to the reference plane that bisects it. For this reason the guided modes can be classified in even or odd modes. The mode which profile has the lowest frequency and fewest nodes is the fundamental mode. One characteristic of this mode is that it is always an even band.

In one hand, a waveguide can be single mode in a particular range of frequencies. In order to avoid the decreasing of the transmission, it is necessary that the guided mode must be within the band gap. The finally of that is avoid losses by the radiation modes, and therefore avoid increases in reflections. On the other hand, multi-modes waveguides and their increasing number of reflections are explained by the coupled theory.

The characteristics mentioned above of the guiding and single modes in a dielectric waveguide are necessary to get high transmission and optical performances in many applications of integrated circuits. However, in absence of photonic band gap (PBG) there are some cases where the transmission is limited by radiation losses.

In this work, strip waveguide with holes and corrugated waveguides were the structures used for the analysis of slow light behavior. As we have mentioned these structures were modeled with the MPB software and the FDTD solutions software.

1.10.1.- Strip waveguide with holes.

Strip waveguide with holes is a periodic structure formed by a strip waveguide where cylindrical holes are introduced in a periodic manner. The holes have a spacing a (lattice constant), radius r and the width of the waveguide w_i, see Figure 1.9. The structure is surrounded by a medium with refractive index lower than the structure.

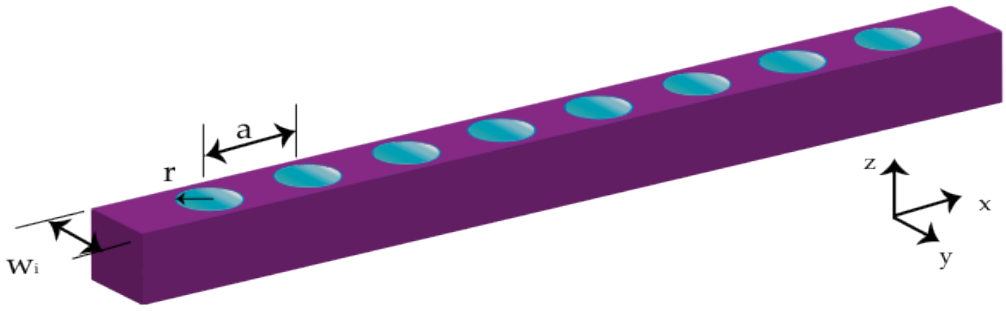

Figure 1.9.- Strip waveguide with holes. With The geometrical parameters are: lattice constant a, hole radius r and the width w_i.

The propagation mechanism in this structure is very similar to that in the nanopillars structure: the space between the holes is the place where the EM field is mainly confined, which act as cavities. But now, continuity between high index regions makes a wider PBG to appear for TE modes *(S. Fan J. W., 1995)*. The bands become flat in the edge of the First Zone of Brillouin.

1.10.2.- Corrugated waveguide.

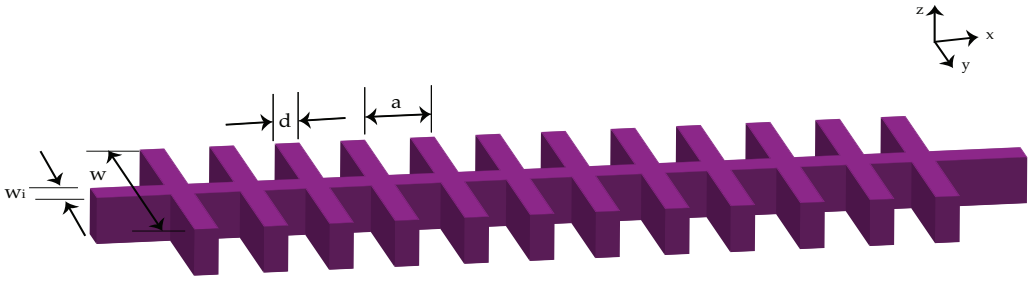

Figure 1.10.- Corrugated waveguide. Which the geometrical parameters are: a as lattice constant, width of strip w_i, length of corrugations w and d width of corrugations.

Corrugated waveguide is a structure which periodicity consist in periodic transversal elements with the parameter *a* as period, width of strip w_i, length of corrugations *w* and *d* width of corrugations, see Figure 1.10.

The expected advantages are the same as those expected for the waveguide with adjacent rods: a greater index change due to the linear effects and a highly efficient coupling of light from/to the access strip waveguide, *(Jaime García, 2008)*.

1.11.- References

- Alessandro Massaro, *Photonic crystals introduction, applications and theory*. InTech, (2012).
- Azzedine Boudrioua, *Photonic waveguides theory and applications*. Wiley, (2009).
- Charles Kittel, *Introduction to solid state physics* (Seventh ed.). Wiley, (1996).
- Eli Yablonovitch, Inhibited spontaneous emission in solid-state physics and electronics. *Physics Review Letter* ***58*** *2059*, 2059–2062, (1987).
- Eugene Hecht, *Optics* (Third ed.). (R. D. Col, Trans.) Addison Wesley Iberoamericana, (2000).
- John D. Joannopoulos, R. D. Meade & J. N. Winn, *Photonic Crystals: Molding the Flow of Light* (First ed.). Princeton University Press, (1995).
- Jaime García, P. Sanchis, *et al.,* 1D periodic structures for slow-wave induced non-linearity enhancement. *Optics Express* ***16*** (5), 3146-3160, (2008).
- Jean-Michel Lourtioz, Henry Benisty, *et al., Photonic crystals towards nanoscale photonic devices*. (P. N. Favennec, Trans.) Springer, (2005).
- John D. Joannopoulos, Steve G. Johnson, *et al., Photonic crystals: Molding the flow of light* (second ed.). Princeton University Press, (2008).
- Kane S. Yee, Numerical solution of initial boundary value problems involving Maxwell's equations in isotropic media. *IEEE Transactions on Antennas and Propagation* ***14*** (3), 302-307, (1966).
- Kazuaki Sadoka, *Optical properties of photonic crystals*. Springer, (2001).

- Thomas F. Krauss, Richard M. De La Rue, *et al.,* Two-dimensional photonic-bandgap structures operating at near-infrared wavelengths. *Letters to Nature* ***383***, 699 – 702, (1996).
- K. Busch, Photonic band structure theory: assessment and perspectives. *Compte Rendus Physique* ***3***, 53-66, (2002).
- M. Miyagi, S. Nishida, Transmission characteristics of dielectric tube leaky waveguide. *IEEE Transactions on Microwave Theory and Techniques* ***28***, 536-541, (1980).
- Mikhail A. Noginov, Graeme Dewar, *et al., Tutorial in complex photonic media,* SPIE Press Books **PM194**, (2009).
- Mohamad Azadeh, *Fiber optics engineering*. (B. Mukherjee, Ed.) Springer, (2009).
- R. H. Lipson, C. Lu Photonic crystals: a unique partnership between light and matter. *European Journal of Physics* ***30*** (4), (2009).
- Sajeev John; Strong localization of photons in certain disordered dielectric superlattices. *Physics Review Letter* ***58***, 2486–2489, (1987).
- S. Fan, J. Winn, *et al.,* Guided and defect modes in periodic dielectric waveguides. *Journal of Optical Society of America B* ***12*** (7), 1267-272, (1995).
- S. Fan, P. R. Villenueve, *et al.,* Design of three-dimensional photonic crystals at submicron length scales. *Applied Physic Letter* ***65*** (11), 1466–1468, (1994).
- S. González García, A. Rubio Bretones, *et al.,* Finite difference time domain methods. In D. Poljak, *Time Domain Techniques in Computational Electromagnetics*. Spain: WIT Press, (2004).

Chapter 2.- Slow Light and extrinsic losses.

2.1.- Introduction.

In this section we analyzed the transmission and losses of our structures in the slow-light regimen: strip waveguide with holes and corrugated waveguide. For this reason we analyze slow-light basic concepts necessary to understand and study this phenomenon. We also examine losses in these systems, especially those caused by technological imperfections in the fabricated devices, known as extrinsic losses. As we will see backscattering scales quadratically with the group index, n_g^2, hence this type of losses is a limitation in some slow-light devices.

2.2.- Slow light.

Slow light is a physical phenomenon where the light is propagated in a medium with low group velocity (v_g), more specifically, $v_g << c$, where c is the light velocity in the medium. This phenomenon produces a high light-matter interaction, which offers additional control over of the spectral bandwidth of this interaction. Also it allows us to delay and temporarily store light in all-optical memories, *(T. F. Krauss, 2008)*. Other consequence is enhancement of the linear effects, such as gain, termo-optic and electro optic.

The interactions between photons and transparent matter are not strong; as consequence, the lasers of high power are required for breaking this limitation and induce non-linear responses. The slow-light phenomenon can enhancement of nonlinear effects too. For example, for nonlinear effect such as Kerr effect, in the regimen of slow light, when a pulse enters

in a photonic crystal waveguide, the front of the pulse will moves slower than its back. So the back of pulse attains the front of it, therefore the pulse will be spatially compressed and as result its energy density is increased. See Figure 2. 1, *(T. F. Krauss, 2007)*. Nonlinear effects are scaled with the slow-down factor of the waveguide, because the nonlinear effects depend on the density of energy.

Slow light has been observed in many experiments, such as that reported in 1999 by Hau group, where a $v_g << 17 m/s$ was obtained. As the author quoted: *"Observation of light pulses propagating at a speed no faster than a swiftly moving bicycle . . . comes as a surprise"*, (Hau, 1999).

When the spectrum of a pulse is near to a bandgap edge and the dispersion curve reaches a turning point, then v_g can be reduced to zero. But in the slow light regimen the dispersion can be significant and it modifies the light propagation.

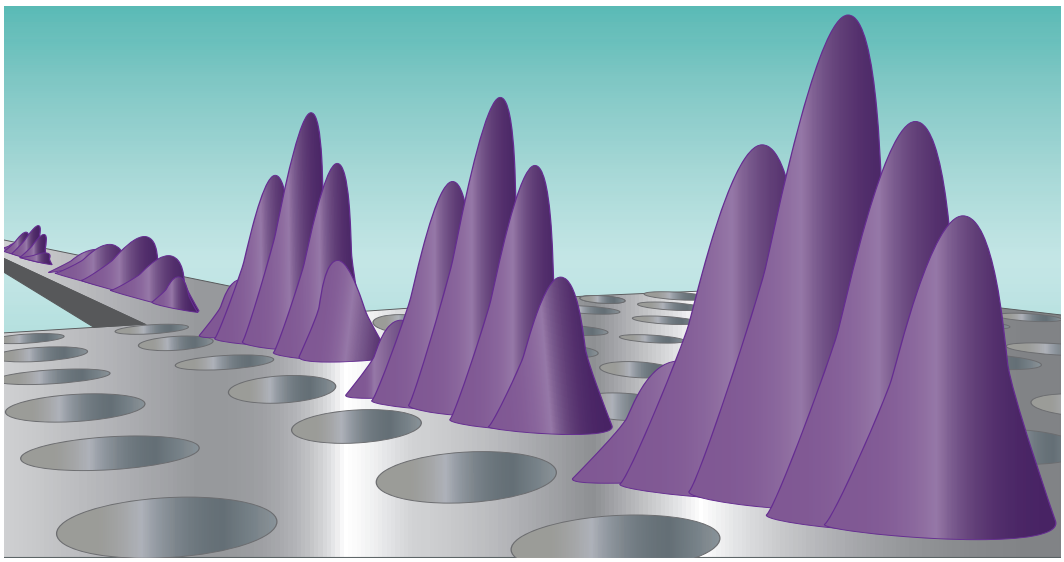

Figure 2. 1.- A pulse in the slow light regimen is compressed and thus its energy density is increased. Nonlinear effects are scaled with the slow-down factor of the structure; in this case the Kerr effect is enhanced.

However, the slow light dispersion can be controlled in specially designed structures and the benefits of this phenomenon can be used, *(A. Figotin, 2005), (M. Ibanescu, 2004), (A. A. Sukhorukov, 2007)*. In photonic crystals the slow light is related with high dispersion, so almost all the benefits are weaken up and the bandwidth of work is severally limited. But this is subject to the geometrical design of each structure. A good or bad design allows to enjoy or not to enjoy the benefits of that phenomenon. For this aim, good understanding of slow light can help to overcome the dispersion limitations, *(Eich, 2004), (Lars H. Frandsen, 2006)*.

Nowadays, slow light is a field with a wide spectrum of applications and potential applications. It is considered as a versatile phenomenon because its practical implementation can be used in many technologies, such as photonic crystals devices, low-loss optical waveguides, optical switches, techniques of micro-fabrication and others.

2.3.- Slow light concepts.

Let us consider a monochromatic plane wave of amplitude E_0 and angular frequency ω, traveling through a medium with refractive index $n(\omega)$, given by Eq. (2.2). For simplicity, we consider that the wave travels in the z direction. It will be assumed that there is not absorption, so the wave vector $k(\omega)$ can be written as:

$$k(\omega) = \frac{n(\omega)\omega}{c}, \qquad (2.1)$$

and the electric field:

$$E(z,t) = E_0 e^{i\varphi}. \qquad (2.2)$$

The phase φ for the last equation, which value is assumed to be constant, is:

$$\varphi = (kz - \omega t). \tag{2.3}$$

If it is regarded a phase motion in the space $\Delta z = z_1 - z_0$ at time $\Delta t = t_1 - t_0$, for the value $\varphi = 0$, from expression Eq. (2.3) we obtained:

$$k\Delta z - \omega\Delta t = 0 \tag{2.4}$$

and the propagation phase speed $v_p = \frac{\Delta z}{\Delta t}$, from the last relation is:

$$v_p = \frac{\Delta z}{\Delta t} = \frac{\omega}{k} \tag{2.5}$$

also v_p is equal too

$$v_p = \frac{c}{n} = \frac{\omega}{k}. \tag{2.6}$$

Considering that the phase φ doesn´t change as a function of ω, *(Robert W. Boyd, 2002)*. This implies that $\frac{d\varphi}{d\omega} = 0$, substituting Eq. (2.1) in Eq. (2.3), and taking its first derivate.

$$\frac{d}{d\omega}\varphi = \frac{d}{d\omega}\left(\frac{n(\omega)\omega}{c}z - \omega t\right) = 0 \tag{2.7}$$

$$\frac{d\varphi}{d\omega} = \frac{dn(\omega)}{d\omega}\frac{\omega z}{c} + \frac{n(\omega)z}{c} - t = 0 \tag{2.8}$$

$$\frac{dn(\omega)}{d\omega}\frac{\omega z}{c} + \frac{n(\omega)z}{c} = t \tag{2.9}$$

The group velocity v_g is defined as $v_g = \frac{z}{t}$ and, then using the last expression, it is possible rewritten it as:

$$v_g = \frac{c}{\frac{dn(\omega)}{d\omega}\omega + n(\omega)} \tag{2.10}$$

Now, considering the first derivate to equation Eq. (2.1).

$$\frac{dk(\omega)}{d\omega} = \frac{dn(\omega)}{d\omega}\frac{\omega}{c} + \frac{n(\omega)}{c} \tag{2.11}$$

$$\frac{d\omega}{dk(\omega)} = \frac{c}{\frac{dn(\omega)}{d\omega}\omega + n(\omega)} \tag{2.12}$$

So, the comparison of equation Eq. (2.12) and Eq. (2.10) gives:

$$v_g = \frac{c}{\frac{dn(\omega)}{d\omega}\omega + n(\omega)} = \frac{d\omega}{dk(\omega)} \tag{2.13}$$

The group velocity can be expressed too in terms of group index n_g as

$$v_g = \frac{c}{n_g}, \tag{2.14}$$

where,

$$n_g = n(\omega) + \frac{dn(\omega)}{d\omega}\omega. \tag{2.15}$$

While to get slow light is required a positive and large value of $\frac{dn(\omega)}{d\omega}$ on the right hand side of Eq. (2.15). A positive value of that is called as *normal dispersion*, whereas a negative value is known as *anomalous dispersion*. Also, it is observed too, that $\frac{dn(\omega)}{d\omega}$ is the term which makes different

group index from phase index, *(Mikhail A. Noginov G. D., 2009), (Robert W. Boyd, 2002).*

Slow or fast light can be generated because in the optical regimen the frequency ω is very large. Small or large values of v_g can be produced by any method or technique that increases the dispersion magnitude.

2.4.- Group velocity dispersion.

When a pulse is traveling through a strip waveguide or a photonic crystal waveguide, its phase fronts travel with the velocity v_p. But the pulse centers travel with the v_g velocity. Because the pulse has different frequency components, they must travel with different group velocities and, as consequence, its shape is modified, *(Jan-MichaelBrosi, 2009)*.

An interesting effect of the Slow light phenomenon is the pulse distortion. Pulses can propagate in a highly dispersive medium with small pulse distortion effects. The propagation constant $k(\omega)$ is expanded in a Taylor series around $\omega = \omega_0$ to carry out a distortion effect analysis,. Through this, it is possible to generate the phase velocity and the group velocity terms.

$$k(\omega) = k_0(\omega_0) + k_1(\omega_0)(\omega - \omega_0) + \frac{k_2}{2}(\omega_0)(\omega - \omega_0)^2 + \frac{k_3}{6}(\omega_0)(\omega - \omega_0)^3 + \ldots \quad (2.16)$$

where $k_j = \left(\frac{d^j k}{d\omega^j} \right)_{\omega=\omega_0}$, and

$$k_0 = k_0(\omega_0) \quad (2.17)$$

k_0 is known as the wave vector magnitude of the optical pulse. The inverse of the group velocity is:

$$k_1(\omega_0)=\left(\frac{dk}{d\omega}\right)_{\omega=\omega_0}=\frac{n_g}{c}=\frac{1}{v_g}, \tag{2.18}$$

and finally, the number $k_2(\omega_0)$ is known as Group Velocity Dispersion (GVD) or chromatic dispersion.

$$k_2(\omega_0)=\left(\frac{d^2k}{d\omega^2}\right)_{\omega=\omega_0}=\frac{d}{d\omega}\left(\frac{1}{v_g}\right)_{\omega=\omega_0}=\left(-\frac{1}{v_g^2}\frac{dv_g}{d\omega}\right)_{\omega=\omega_0}=\frac{1}{c}\frac{dn_g}{d\omega} \tag{2.19}$$

Number $k_2(\omega_0)$ measures the dispersion of the v_g. If $k_2(\omega_0)$ has a positive value, short wavelength component of a pulse is propagated slower than long wavelength component, and vice versa.

In the dispersion diagram, a band which slope is near to zero implies values of v_g that tend to zero. Modes in Photonic crystals waveguides (PC-WGs) can exhibit regions with very low group velocity and very high chromatic dispersion, *(M. Notomi K. Y., 2001)*.

2.5.- Dispersion in waveguides.

Waveguide dispersion occurs when part of the energy of a mode propagates through the core and other part travels in the cladding. The radiation between these two energies depend on the wavelength, and as a consequence index variations with the frequencies are generated. As the refractive index of cladding is lower than that of the core, there is energy spread in such a way that the energy travel faster in the cladding, *(Mohamad Azadeh, 2009)*.

Material dispersion takes place when the refractive index of certain material depends on the frequency ω. The material dispersion results on spreading of the signal, this is due to finite spectral width of the signal. In almost all optical fibers this dispersion type is the main source of chromatic dispersion.

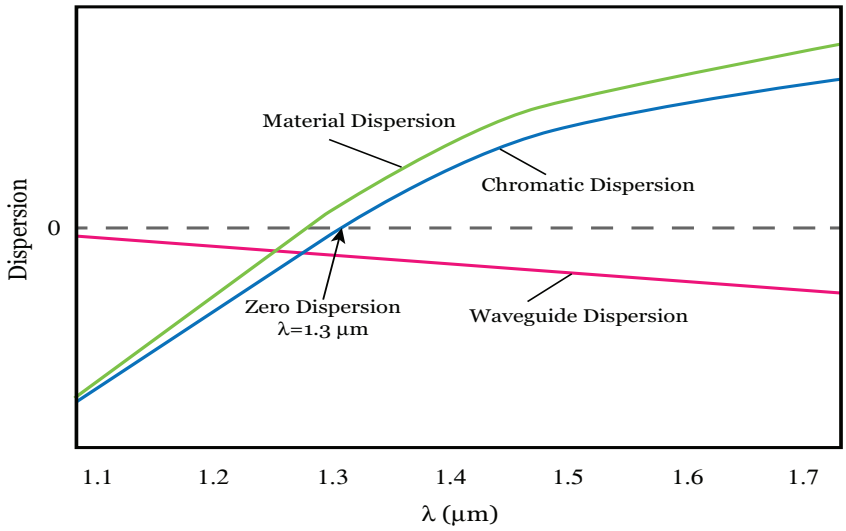

Figure 2. 2.- Chromatic dispersion consist of material and waveguide dispersion. Two phenomena produce opposite effects. For silica glass the zero chromatic dispersion happens for $\lambda = 1.3$ ***μm.***

Two types of dispersion integrate the dispersion parameter or chromatic dispersion: waveguide and material dispersion, see Figure 2. 2. In this phenomenon, different components of a pulse move with distinct velocities. The chromatic dispersion is defined as:

$$D = -\frac{2\pi c}{\lambda^2} k_2, \qquad (2.20)$$

where λ is the wavelength in the vacuum and k_2 is given by (2.19).

In a monomode and multimode fibers, chromatic dispersion occurs because light of different wavelengths is transported at distinct velocities

through of the fiber. Some wavelengths arrive to the end of the fiber before than others, which mean that there is a delay in time. This dispersion is measured using such time delays.

In telecommunications, the chromatic dispersion is a factor that limits the information carried along of waveguides and fibers, because it causes bit errors in digital information or distortion.

2.6.- Losses in photonic crystals.

The photonic crystals as periodic media possess unique properties of light scattering *(Kazuaki Sakoda, 2001)*. The features of the propagation of the light and confinement of this, at wavelength scale, are defined by the scattering. Large propagation losses are yield in photonic crystals waveguides are caused by their complex geometrical shapes, such as the strong light scattering at the imperfections of the fabricated structures.

In the PCs an uncontrolled scattering can produce losses of light transmission. Although, with an adequate geometrical design is possible to taylor the scattering effects, so the benefits of the PCs in a diversity of novel applications, such as the optical switches for the slow-light phenomenon, can be used. The problem is quite promising because all the technological advances in PC waveguides, however, the loss mechanisms research in photonic crystals waveguides is still incipient, but it is expected that this will be fundamentally different from that of conventional waveguides *(D. Marcuse, 1974)*. It is generally believed that loss scales as $1/v_g$ can be achieved *(Y. Takana, 2004)*.

Nowadays, Silicon-On-Insulator (SOI) is a material that has been extensively used in the investigation of the integrated optical components.

These devices are fabricated with the same microchips processes. The high index contrast of SOI with air or glass allows to strongly confine fields in the waveguides and also allows to build photonic crystals. These structures can be designed to have a complete photonic band gap. But the losses are a limitation to these devices.

The high index contrast with air or glass in the structures imperfections produce a strong scattering of light. Recently, several studies have showed a significant loss reduction in light propagation, with this, a great advance in fabrication technology of SOI has been achieved, *(Sharee McNab, 2003), (Yoshimasa Sugimoto, 2004), (M. Notomi A. S., 2004).* For example: The losses for a SOI strip waveguide of width of the strip $w = 500$ nm and of height $h = 220$ nm are $2.4\,{}^{dB}\!/_{cm}$, *(P. Dumon, 2004)*.

For a better understanding of the loss propagation in photonic crystal waveguides, its study has being divided in intrinsic and extrinsic losses. The intrinsic scattering losses are losses caused by inherently leaky modes, *(H. Benisty, 2001), (L. C. Andreani M. A., 2003), (W. Bogaerts, 2001).* While, extrinsic scattering losses are due to random fabrication variations, such as disorder and surface roughness, *(S. Hughes, 2005)*.

First, let is go to some of the basic loss mechanism descriptions. The Beer-Lambert law explains the light attenuation of a beam while this travels through of an absorbing material (device) of length L.

$$I = I_0 Exp[-\alpha L], \tag{2.21}$$

where α is the attenuation coefficient, I_0 is the input intensity and I is the output intensity.

This law is just applicable in the processes where the light absorption is toward the propagation direction of the mode and the light cannot return

to the input point. Then in multiple scattering, more specifically in the backscattering, the Beer Lambert don´t apply, *(M. Patterson, 2009)*.

However, in order to introduce a description that include intrinsic and extrinsic losses we need an expansion of the attenuation coefficient α in function of n_g, *(Thomas F. Krauss, 2010)*. The intrinsic and extrinsic losses can be expressed by:

$$\alpha = c_0 + c_1 n_g \gamma + c_2 n_g^2 \rho, \tag{2.22}$$

where c_0 express the intrinsic losses, ρ contains the hole shape effects, γ described the mode shape effects, c_1 and c_2 are parameters determined by the technological quality of the devices, *(Thomas F. Krauss, 2010)*. The extrinsic expressions for γ and ρ and the intrinsic losses will be explain in the following sections.

2.7.- Intrinsic losses.

Intrinsic losses are inherent losses of the waveguides. When the TIR is not satisfied there are leakage losses of the modes that move toward out of the slab material.

In silicon, there are two types of intrinsic losses: linear and nonlinear material losses. The linear material losses of silicon are negligible, *(E. D. Palik, 1998)*. The main nonlinear losses are the free-carrier-absorption (FCA) and the two-photon absorption (TPA) *(H. K. Tsang, 2004)*.

The light-line is quite an useful concept to understand the intrinsic losses. The light-line is a concept used in the dispersion diagrams in order to

distinguish the guided and the radiated modes. This line depends on the structure geometry and it separates the region of the discrete guided modes and the forbidden region, where there are continuum radiation modes. If the modes of the PC waveguide are below the light-line (of the substrate and the cover material) the TIR condition is met. In this case, the structure works as ideal PC waveguide and there are not leakage losses, *(Jan-Michael Brosi, 2009)*. However, there are radiative modes, and thereby significant losses, when the modes cross the light line, *(P. Lalanne, 2002)*, *(L. C. Andreani M. A., 2003)*.

The light-line depicted the dispersion of a wave that travels through of a medium with refractive index n_2. The line-line expressions of the light-line are showed by Eq. (2.23) and Eq. (2.24). Those modes are lying above the line and they are affected by intrinsic radiation losses due to out of plane diffraction.

$$k = \frac{\omega n_2}{c}, \tag{2.23}$$

$$\omega = \frac{kc}{n_2}. \tag{2.24}$$

The light-line depends of the higher refractive index n_2 of the device. When the light-line is surpassed are originated radiation modes. When the light-line is surpassed the radiation modes are originated. The higher the background index of a Photonic crystal waveguide (PC-WG) is smaller of both, low-loss frequency and wave vector range of the waveguide (WG) mode. Therefore it is desirable to choose a low background index, like e. g. the air, *(Jan-Michael Brosi, 2009)*.

The light line intrinsically limits the application of photonic crystals. Then, the knowledge about intrinsic losses dependence on PCs parameters can help to quantify of the losses level and thereby improve the structures design.

2.8.- Extrinsic losses.

In the design, the photonic crystals are tailored as ideal structures, but in the fabrication, let's be realistic. In the fabrication process there are defects by random fabrication variation in the structures. Such defects cause a type of losses known as extrinsic losses.

Some factors that contribute to extrinsic losses are: insufficient etch depth, roughness, non-vertical sidewalls, non-vertical shape of the holes, and disorder, such as in hole centers or hole radius, and material inhomogenities as well, *(S. Hughes, 2005)*.

The extrinsic losses are integrated by two types of losses: Backscattering with α_{back} as loss factor, and out of plane radiation, with α_{out} as loss factor, see Figure 2. 3; *(S. G. Johnson M. P., 2005), (L. C. Andreani D. G., 2007)*.

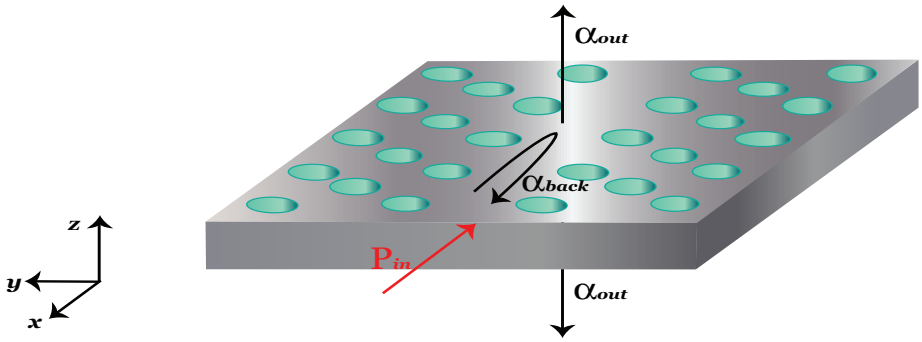

Figure 2. 3.- Photonic crystal waveguide type w_1 ***where the incident power*** P_{in} ***can be scattered back in counter propagation and/ out of plane, with the loss factors*** α_{back} ***and*** α_{out} ***respectively.***

The backscattering is a problem for any waveguide type, it has been observed and expected to scales as n_g^2, *(E. Kuramochi, 2005), (S. Hughes, 2005)*. The scaling n_g^2 of backscattering is a serious limitation for the slow

light regimen (high values of group index), such as PCs with short length of transmission.

When the losses are studied, the mode shape on the group index n_g is a parameter that gives information about the fraction of field available for scattering at imperfections and also determines the strength of the field in the holes sidewall, *(L. O'Faolain S. A., 2010)*. The extrinsic losses contribution to the modes is modeled by the following expression:

$$\alpha = c_1 \gamma n_g + c_2 \rho n_g^2 \tag{2.25}$$

Where the mode shape contributions to out of plane (radiation) losses and backscattering losses are defined by $\gamma = \gamma(k)$ and $\rho = \rho(k)$, respectively. The group index n_g and, the coefficients c_1 and c_2 that give information about the technological parameters, *(S. Mazoyer, 2009)*, such as sidewall roughness, sidewall angle, hole position variations or/and hole size variations. They are independent of geometrical design.

Backscattering losses are present in the devices when the guided mode is propagated backwards. This type of extrinsic losses only appears in single mode systems. The mode shape depends on backscattering parameter ρ. The backscattering is given by the expression (2.26). Here, it is assumed that the scatterers behave as radiating dipoles, based on the Lorentz reciprocity theorem, *(B. Wang, 2008)*. In this equation, it is supposed that the disorder arises in the sidewalls.

$$\rho = \sum_n \left| \int_{L_c} \vec{E}_T \cdot \vec{E}_T + \left(\varepsilon_1 \varepsilon_2\right)^{-1} \vec{D}_N \cdot \vec{D}_N \, d\vec{r} \right|^2, \tag{2.26}$$

where $\vec{E}_T$ is the electric field component tangential to the surface of the hole, $\vec{D}_N$ is the displacement field component normal to surface of hole,

these fields are continuous across of the surface. ε_1 and ε_2 are the dielectric constants of the device. The correlation length L_c is measured along the boundaries of hole. In an unit cell, n is the number of parts of the L_c.

The out of plane radiation losses, γ, appears in a continuum of radiation modes. Here, there is a coupling between continuum radiation modes and the Bloch mode. The disorder is analyzed as local dipole sources and it is assumed that coupling of the dipole radiation to the air-mode is independent of the position and wavelength λ an expression for γ is obtained:

$$\gamma = \sum_{n} \left| \int_{L_c} \vec{E}_T + \left(\varepsilon_1\right)^{-1} \vec{D}_N \, d\vec{r} \right|^2 , \qquad (2.27)$$

where the parameters are the same that the backscattering case. ε_1 considers local field corrections and the local phase of the component fields, *(L. O'Faolain S. A., 2010)*.

In this work the extrinsic losses will be analyzed using a code developed by the Thomas Krauss group of the Massachusetts Institute of Technology (MIT) *(L. O'Faolain S. A., 2010)*, based on MIT Photonic bands (MPB) which use the plane wave expansion.

2.9.- References

- A. Sukhorukov, *et al., Slow light with flat or offset band edges in few-mode fiber with two gratings* **15**, Optics Express (2007).
- Figotin, *et al.,* Gigantic transmission bandedge resonance in periodic stacks of anisotropic layers. *Physics Review E, **72***, (2005).
- Yu. Petrov, *et al., Zero dispersion at small group velocities in photonic crystal waveguides* Applied Physics Letters **85**, (2004).
- Alex Figotin, *et al., Gigantic transmission bandedge resonance in periodic stacks of anisotropic layers* Physics Review E **72**, (2005).
- Wang, *et al.,* Backscattering in monomode periodic waveguides. *Physics Review B **78*** (24), 245108-245116, (2008).
- Gerace, *et al.,* Disorder-induced losses in photonic crystal waveguides with line defects. *Optics Letters **29***, 1897-1900, (2004).
- Marcuse, (1974). *Theory of Dielectric Waveguides*. Academic, New York.
- Mikhail A. Noginov, *et al., Tutorials in complex photonic media*. SPIE Press, (2009).
- Kuramochi, *et al.,* Disorder-induced scattering loss of line-defect waveguides in photonic crystal slabs. *Physics Review B **72***, 161318-161322, (2005).
- D. Palik, *Handbook of Optical Constants of Solids*. San Diego, CA: Academic Press, (1998).
- Benisty, *et al.,* Out-of-plane losses of two-dimensional photonic crystals waveguides: Electromagnetic analysis. *Journal of Applied Physics **89***, 1512-1515, (2001).
- K. Tsang, *et al.,* Role of free carriers from two-photon absorption in Raman amplification in silicon-on-insulator waveguides. *Applied Physics Letters **84***, 2745-2747, (2004).
- Jan-Michael Brosi, *Slow-Light Photonic Crystal Devices for High-Speed Optical Signal Processing **4***. Karlsruhe Series in Photonics & Communications, (2009).

- Kazuaki Sakoda, *Optical Properties of Photonic Crystals*. Berlin: Springer, (2001).
- L. C. Andreani, *et al.,* Light–matter interaction in photonic crystal slabs. *Physica Status Solid B* ***224*** (10), 3528–3539, (2007).
- L. C. Andreani, *et al.,* Intrinsic diffraction losses in photonic crystal waveguides with line defects. *Applied Physics Letters* ***82*** (13), 2011-2013, (2003).
- L. O'Faolain, *et al.,* Loss engineered slow light waveguides. *Optics Express* ***18*** (26), 27627-27638, (2010).
- L. V. Hau, *et al.,* Light speed reduction to 17 metres per second in an ultracold atomic gas. *Nature* ***397***, 594-597, (1999).
- L. V. Hau, *et al., Light speed reduction to 17 metres per second in an ultracold atomic gas,* Letters to Nature ***397***, (1999).
- Lars H. Frandsen, *et al., Photonic crystal waveguides with semi-slow light and tailored dispersion properties*, Optics Express ***14***, (2006).
- M. Ibanescu, *et al., Anomalous dispersion relations by symmetry breaking in axially uniform waveguides,* Physics Review Letter ***92***, (2004).
- M. Notomi, *et al.,* Waveguides, resonators and their coupled elements in photonic crystal slabs. *Optics Express* ***12*** (8), 1551-1561, (2004).
- M. Notomi, *et al.,* Extremely large group-velocity dispersion of line-defect waveguides in photonic crystal slabs. ***87*** (25), 253902-253906, (2001).
- Mohamad Azadeh, *Fiber optics engineering*. Springer, (2009).
- M. Patterson, *et al.,* Disorder-induced incoherent scattering losses in photonic crystal waveguides: Bloch mode reshaping, multiple scattering, and breakdown of the Beer-Lambert law. *Physical Review B* ***80*** (19), 195305-195311, (2009).
- P. Dumon, *et al.,* Low-loss SOI photonic wires and ring resonators fabricated with deep UV lithography. *Photonics Technology Letters IEEE* ***16*** (5), 1328 – 1330, (2004).

- P. Lalanne, Electromagnetic analysis of photonic crystal waveguides operating above the light cone. *IEEE Journal of Quantum Electronics* ***38*** (7), 800-804, (2002).
- Robert W. Boyd, *et al.,* "slow" and "fast" light. In E. Wolf, *Progress in optics* ***43,*** 497-530, (2002).
- S. G. Johnson, *et al.,* Roughness losses and volume-current methods in photonic-crystal waveguides. *Applied Physics B* ***81*** (2-3), 283-293, (2005).
- S. Hughes, *et al.,* Extrinsic Optical Scattering Loss in Photonic Crystal Waveguides: Role of Fabrication Disorder and Photon Group Velocity. *sPhysics Review Letter* ***94*** (3), 033903- 033907, (2005).
- S. Mazoyer, *et al.,* Disorder-Induced Multiple Scattering in Photonic-Crystal Waveguides. *Physics Review Letters* ***103*** (6), 063903-063907, (2009).
- Sharee McNab, *et al.,* Ultra-low loss photonic integrated circuit with membrane-type photonic crystal waveguides. *Optics Express* ***11***, 2927-2939, (2003).
- T. F. Krauss, *Slow light in photonic crystal waveguides*, Journal of Physics D: Applied Physics ***40***, (2007).
- T. F. Krauss, *Why do we need slow light?* Nature Photonics ***2***, (2008).
- Thomas F. Krauss, *et al.,* Understanding the rich physics of light propagation in slow photonic crystal waveguides. *SPIE Proceedings* ***7612***, 6120L-76120L-9, (2010).
- W. Bogaerts, *et al.,* Out-of-plane scattering in photonic crystal slabs. *IEEE Photonics Technology Letters* ***13***, 565-567, (2001).
- Y. Tanaka, *et al.,* Group velocity dependence of propagation losses in single-line-defect photonic crystal waveguides on GaAs membranes. *Electron Letters* ***40*** (3), 174-176, (2004).
- Yoshimasa Sugimoto, *et al.,* Low propagation loss of 0.76 dB/mm in GaAs-based single-line-defect two-dimensional photonic crystal slab waveguides up to 1 cm in length. *Optics Express* ***12***, 1090-1096, (2004).

Chapter 3.- Results.

3.1.- Introduction.

In this chapter we show our results of the designed and modeled slow light devices: corrugated waveguide and strip waveguide with holes, which geometrical parameters can be fabricated using e-beam or UV photolithography techniques. First, the photonic bands of the slow-light structures were modeled using MPB software. After, we studied the transmission efficiency of these devices using FDTD solutions software. Finally, we carried out a loss analysis, in order to get such loss analysis we used a MPB code of Krauss. We got a value estimate of the success that the fabricated design fulfills the proposed design requirements.

3.2.- Strip waveguide with holes.

The strip waveguide with silica holes to be analyzed is based in SIO single mode waveguide. The periodicity in this structure is created by the introduction of silica holes of radius r, separated a distance a along the propagation direction. This structure is surrounding by silica.

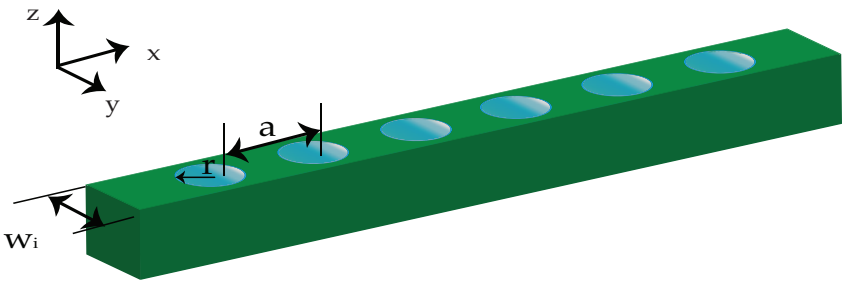

Figure 3. 1.- Strip waveguide with holes in 2D. With The geometrical parameters used in the simulations are: lattice constant $a = 456$ ***nm, hole radius*** $r = 115$ ***nm and the width*** $w_i = 490$ ***nm.***

The geometrical parameters were selected with the aim that the center of the fundamental mode edge in the telecommunications windows, $\lambda = 1550$ nm.

As we will show later the second band seems promising at this wavelength ($\lambda = 1550$ nm), so we modify in several simulations the values of the geometrical parameters until the best values were around this wavelength. The final parameters for the simulations were: $a = 456$ nm, $r = 115$ nm, $w_i = 490$ nm, see Figure 3. 1. The silicon layer has 220 nm of thickness.

However, the selection of the geometrical parameters size is restricted to the technique that would be used in the fabrication process. For example, e-beam (electron beam) lithography posses the better resolution (~ 20 nm) compared with others techniques, such as refractive optical lithography (~ 157 nm) *(Ampere A. Tseng, 2003)*, or UV photolithography (~ 100 nm), *(M. Rothschild, 2005)*. Therefore, we considered that the technique that will use in the fabrication process of our structures would be e-beam lithography.

E-beam lihography offers high precision in the fabricated design (positions and size of elements of the structures), the possibility to reduce the extrinsic losses caused by random variations of the fabrication and achieve high group index n_g, *(OFaolain, 2010)*.

3.2.1.- Dispersion bands.

The numerical analysis of dispersion bands and group index n_g were carried out to using the plane wave expansion (PWE), in particular utilizing the Photonic Bands (MPB) software. This software is a free access one developed by the MIT researchers. The next figure shows dispersion

diagram (frequency as a function of the wave number, in units $2\pi/a$, in the first Brillouin zone) for the first proposed waveguide.

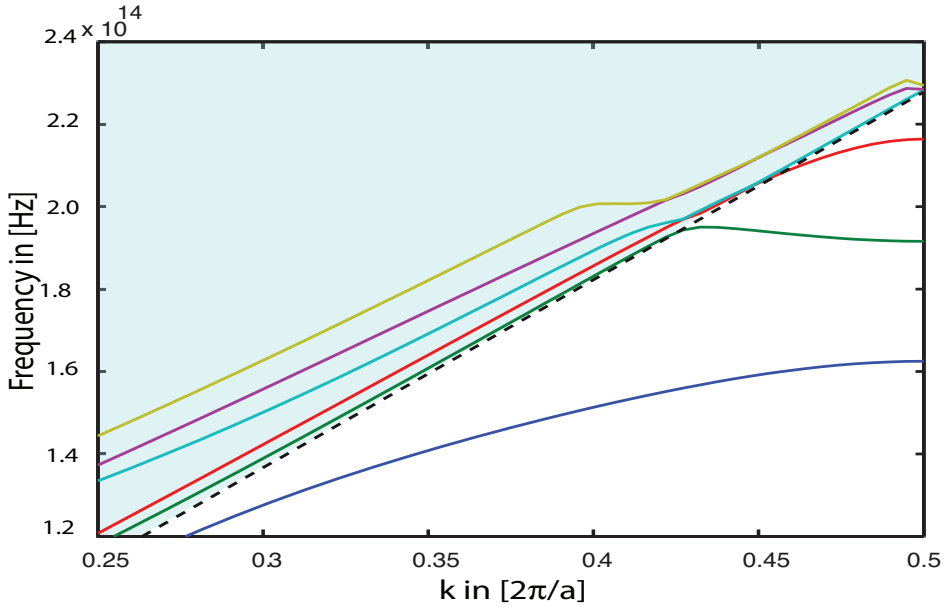

Figure 3. 2.- Dispersion bands of the strip waveguide shown in the figure 3.1. The green line corresponds to second band, in which the TE slow mode propagates at $\lambda = 1550$ nm. The dotted line is the light line. The blue line is the first band, the green one is the second band, the red one is the third band, the cyan one is the fourth band, the magenta one is the fifth and the olive one is the sixth band.

The band of interest in this device is the second band, in which the transversal electric (TE) guided mode propagates around $\lambda = 1550$ nm see Figure 3. 2. The propagation mechanism is explain as following: the electromagnetic field is confinement in the spaces between holes, which act as cavities, (Jaime García, 2008).

3D MPB simulations were utilized to estimate the dispersion bands and group index of this device. The band become flat near to edge of Brillouin zone, this behavior is related to the holes periodicity.

The doted line is the light line. In the right side of this line (white area) are the guided modes, while in the left side (light blue area) are the radiated modes.

As we can observe in the figure for the second band (green line) high values of the group index are present for $k > 0.42$. This also means that slow light phenomenon can take place.

3.2.2.- Group index variations.

In the Figure 3. 3 we have plotted the dependence of the group index as a function of the wavelength for the second band of the proposed structure.

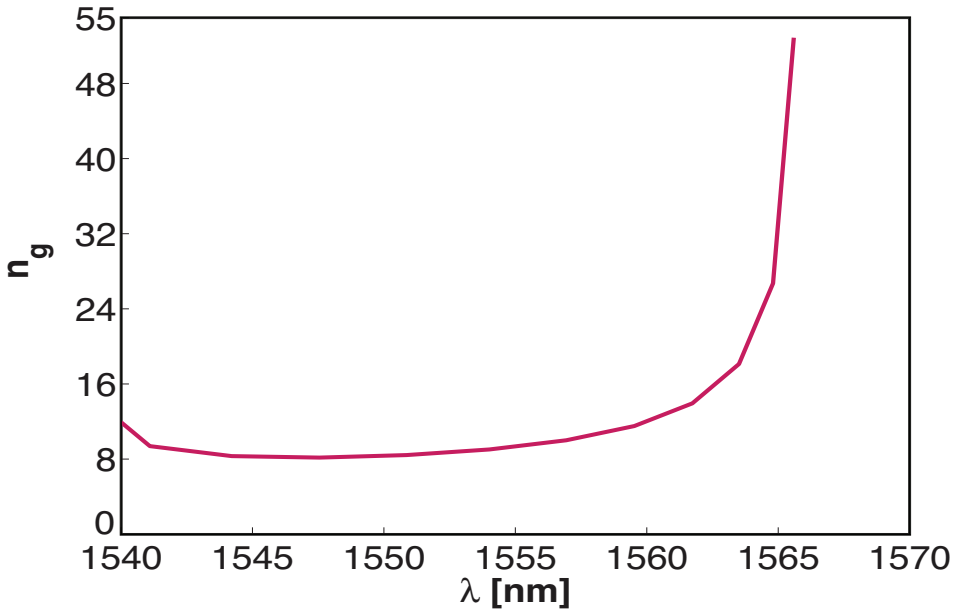

Figure 3. 3 .- Variations of group index as a function of the wavelength for the strip waveguide shown in the Figure 3. 1.

For this device, relatively high values of group index n_g were obtained around $\lambda = 1550$ nm. For this second band, we got a group index constant $n_g \approx 8.5$ with an estimated bandwidth of 14 nm. In direction to the red-

shift the slow light behavior is enhanced, values of $n_g \approx 53$ can be achieved for wavelengths relatively near to the window of the telecommunications.

Also we simulated the group index n_g as a function of the wavelength in the first Brillouin zone for the second band, see Figure 3.4. The Values of group index, n_g, also are calculated using 3D MPB simulations.

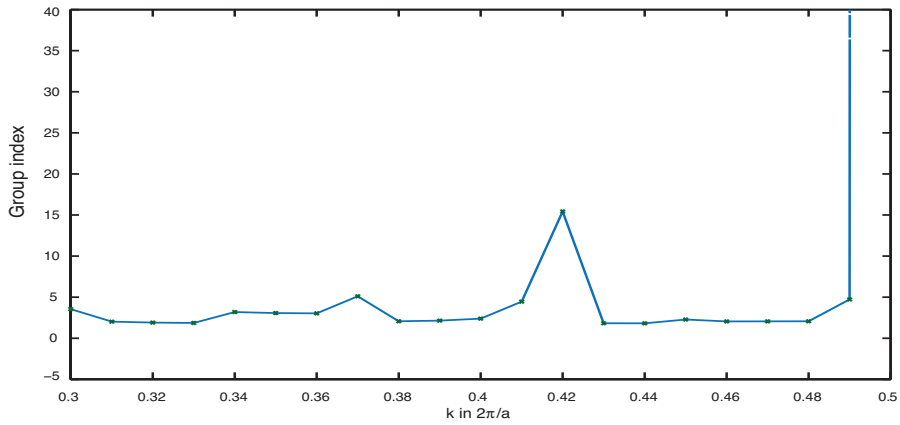

Figure 3. 4.- Group index n_g variations over the first Brillouin zone for the strip waveguide with holes.

As we can observed the group index is relatively constant except in values around $k = 0.42$ where a peak appears. Which is related with the behavior in the dispersion curve for the second band (Figure 3. 2) around $k = 0.42$. Note that for values around $k = 0.49$ in the dispersion band diagram the second band is almost flat (Figure 3. 2), this implies that very large group index values can achieved (see Figure 3.4 for $k = 0.49$). In this region the slow light phenomenon is very strong for the device.

3.2.3.- Transmission and reflection spectra.

The analysis of transmission and reflection spectra were carried out using Finite Difference in Time Domain method, in order to use such method in our analysis we use the commercial FDTD solutions software *(Solutions)*.

We modeled a 3D strip waveguide using such software. The reflection and transmission spectra are normalized to one.

The goal is determine the efficiency of light transmission along of the structure and identify the losses problem due to scattering and/or reflections of light.

In the Figure 3. 5 (a) and Figure 3. 5 (b) are plotted the transmission and reflection spectra for the strip waveguide.

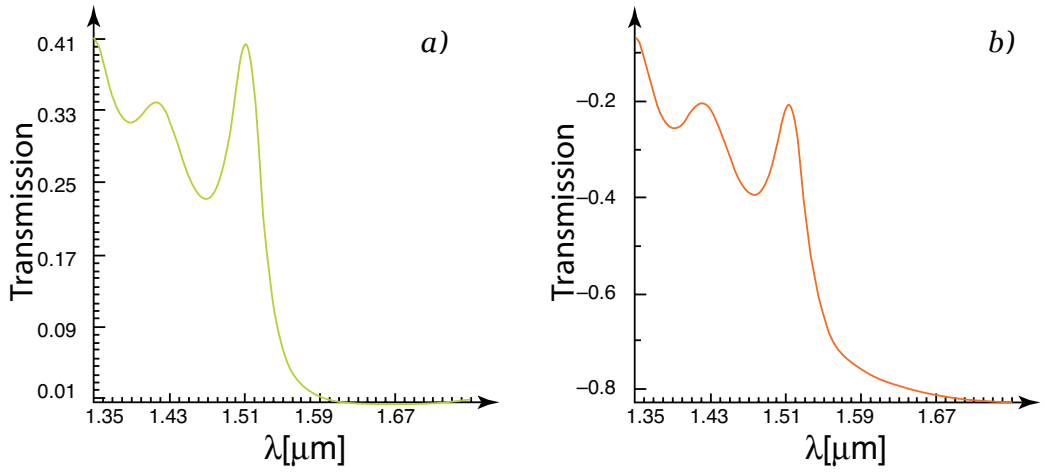

Figure 3. 5 .- a) Transmission and b) reflection spectra for strip waveguide with holes shown in the Figure 3. 1.

We can observe about 41% of transmission and 20% of reflection around $\lambda = 1550$ nm. The nearly abruptly decrease of the transmission around to $\lambda = 1550$ nm is related to the low group velocities in that wavelength (and as consequence we have slow light near to that wavelength).

Let's notice that there are few small ripples in the transmission spectrum. that are related with a Fabry-Perot response of the structure, due to a mismatch between the holes and waveguide modes *(Jaime García, 2008)*. This Fabry-Perot response is caused by residual reflections at the interfaces and lead to decreasing of the transmission.

The Fabry-Perot ripple behavior can be decreased if the mode coupling is improved. A possible technique of mode coupling is using the adiabatic transitions which are implemented by gradually diminishing the steps size of the holes at both ends of the device, but keeping constant the periodicity. The reduction of the periodic elements is equivalent to increase the index refraction of the structure, in this way the band of interest could be shifted up to higher wavelengths, thereby the mode coupling is improved, *(Jaime García, 2008)*.

3.2.4.- Loss analysis.

In chapter II we mentioned that backscattering losses scales as n_g^2, as a serious problem for the slow light structures fabrication. The out of plane scattering losses scales as n_g and it shows a continuum at the radiation modes. On the other hand, Backscattering losses only occurs in mono mode structures where they can be observed as backward propagation of the guided mode. The backscattering losses and out of plane radiation losses, as a function of wave number for the strip waveguide with holes, are plotted in Figure 3. 6. In the Figure 3. 6 (a) the horizontal axis shows the value of the coefficient ρ of the equation (2.25) in the first Brillouin zone, while in the Figure 3. 6 (b) the horizontal axis shows the value of the coefficient γ for the same equation.

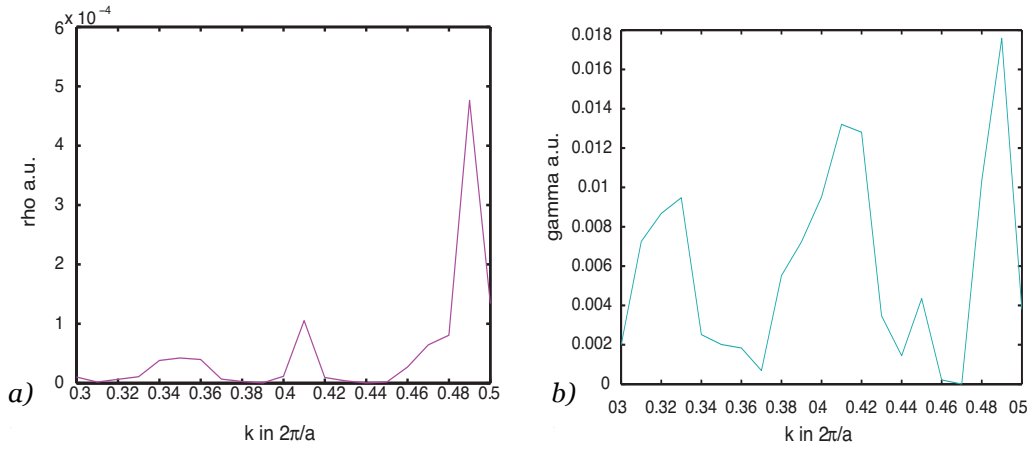

Figure 3. 6.- (a) Backscattering vs k for strip photonic crystal waveguide (b) Out of plane scattering vs k for the strip waveguide with holes.

We observed that the strip waveguide has lower values of backscattering losses in almost all the first Brillouin zone while the larger values are located around $k > 0.49$ with values near to 4.9X10^{-4} dB/cm. This value can be considered very low. The values of out of plane scattering losses are stronger than backscattering as it can be observed in Figure 3. 6. (b). But those values are relatively small, where the largest value of out of plane radiation losses around 0.017 dB/cm.

We observe that from $k = 0.45$ to 0.5, both backscattering and out of plane scattering increase simultaneously. teIn this region the strip waveguide show a flatter band, Figure 3. 2, and this behavior is related with the scaling of backscattering $\left(n_g^2\right)$ and out plane scattering $\left(n_g\right)$ predicted by the theory (L. O'Faolain S. A., 2010). The Figure 3. 7 shows the total losses variations as a function of the wave number k.

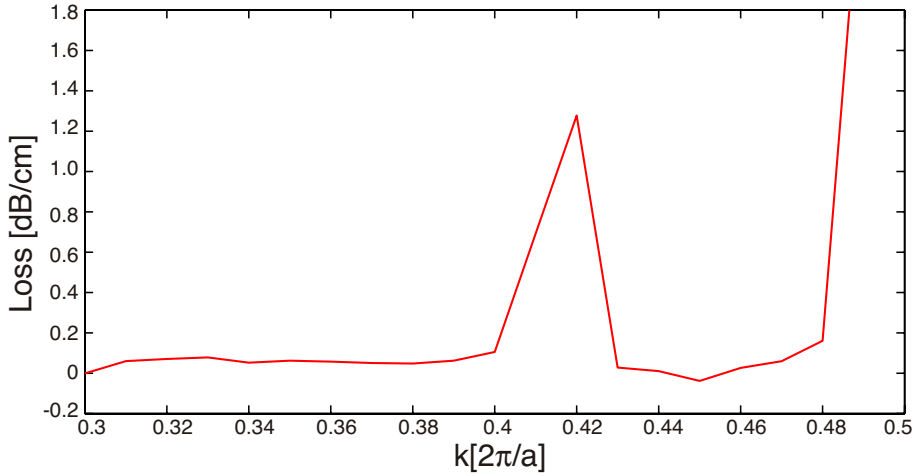

Figure 3. 7.- Total losses variations as a function of the wave number k in the first Brillouin zone for the strip waveguide with holes.

Here we can observe high losses (1.3 dB/cm) around $k = 0.42$ and the higher losses (>1.8 dB/cm) for $k > 0.48$. Note that for region $k > 0.48$ the group index and losses have an almost linear scaling.

Losses around 2 dB/cm are consider as very low losses (M. Notomi, 2007), from our simulations we can observe that for losses near 1.2 dB/cm we can get $n_g \approx 15$ at $k = 0.42$ for the strip waveguide.

3.3.- Corrugated waveguide.

Also, we modeled a corrugated photonic crystal waveguide, surrounded by silica, as the one shown in Figure 3. 8. This structure is created by introducing the periodic transversal corrugations, with lattice constant a. The corrugations have length w and width d; the strip waveguide width is w_i. This structure is relatively easy to fabricate.

In order that the fundamental mode lies around $\lambda = 1550$ nm the geometrical parameters were modified in several simulations. The final geometrical values used in our simulations are: $a = 460$ nm, $d = 210$ nm. $w_i = 380$ nm and $w = 710$ nm. The silicon layer has 220 nm of thickness.

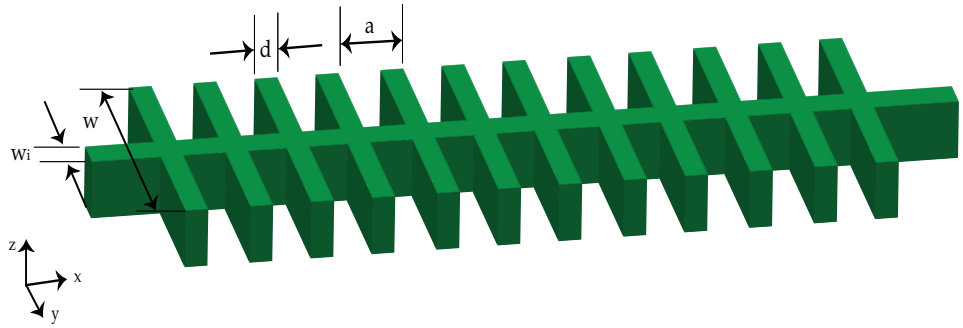

Figure 3. 8.- Corrugated waveguide design in 2D. With The geometrical parameters used in this research are: $d = 210$ ***nm,*** $a = 460$ ***nm,*** $w_i = 380$ ***nm and*** $w = 710$ ***nm.***

3.3.1.- Dispersion bands.

For the numerical analysis of dispersion bands and group index n_g for this structure we used the same software that the same used for the strip waveguide.

In the Figure 3. 9 is plotted the dispersion bands (frequency vs wave number) for the wavelength $\lambda = 1550$ nm.

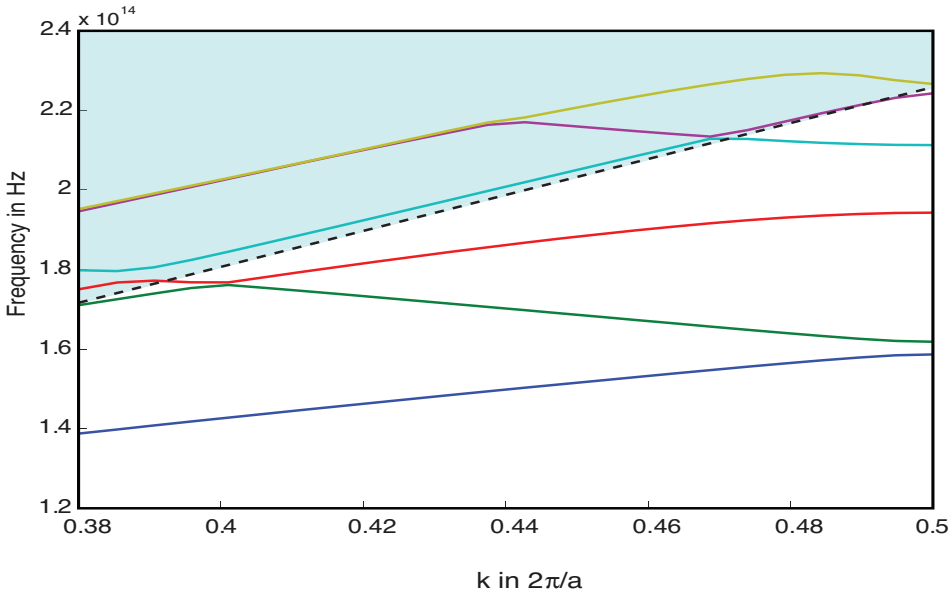

Figure 3. 9.-Dispersion bands of the corrugated waveguide shown in the Figure 3. 8. The blue line corresponds to the first band, the green line corresponds to second one, the red line corresponds to third one and cyan line corresponds and so fort. The dotted line is the light line.

We can observe that the third band (the red line) possess characteristics what made it useful for slow light applications. In a similar way to the strip waveguide, the third band becomes flat near to the frontier of the first zone of Brillouin.

3.3.2.- Group index variations.

In this structure, we observed high values of n_g around $\lambda = 1550$ nm. We found values of group index $n_g \approx 7.8$ for the third band. The slow light behavior, in direction to blue-shift, is enhanced at wavelengths close to $\lambda = 1550$ nm; where high values of the group index ($n_g \approx 23$) can be achieved near to the edge of the third band, see Figure 3. 10.

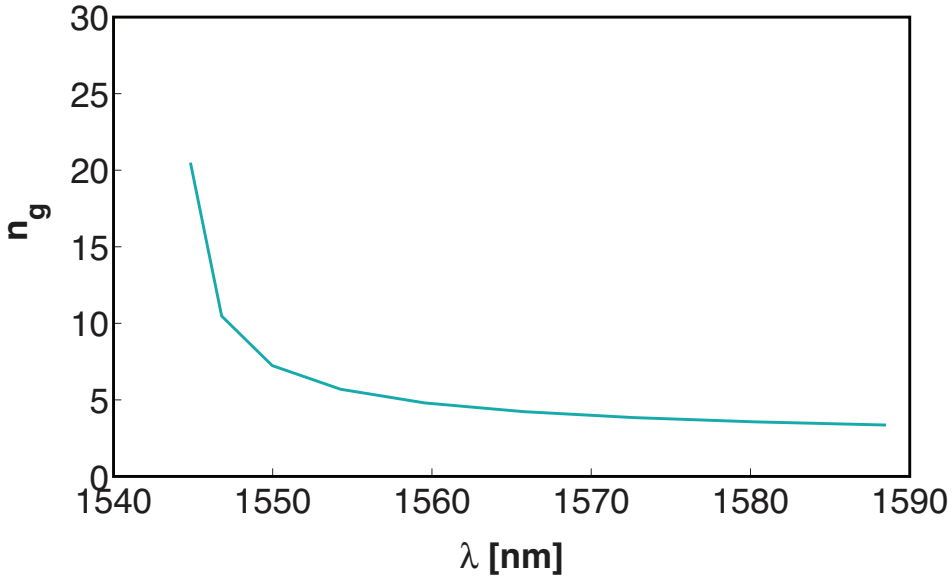

Figure 3. 10.- Variations of group index n_g as a function of the wavelength for the corrugated waveguide shown in the Figure 3. 8.

For this structure we also calculated the group index n_g vs k in the first Brillouin zone. This calculation is plotted in the Figure 3. 11.

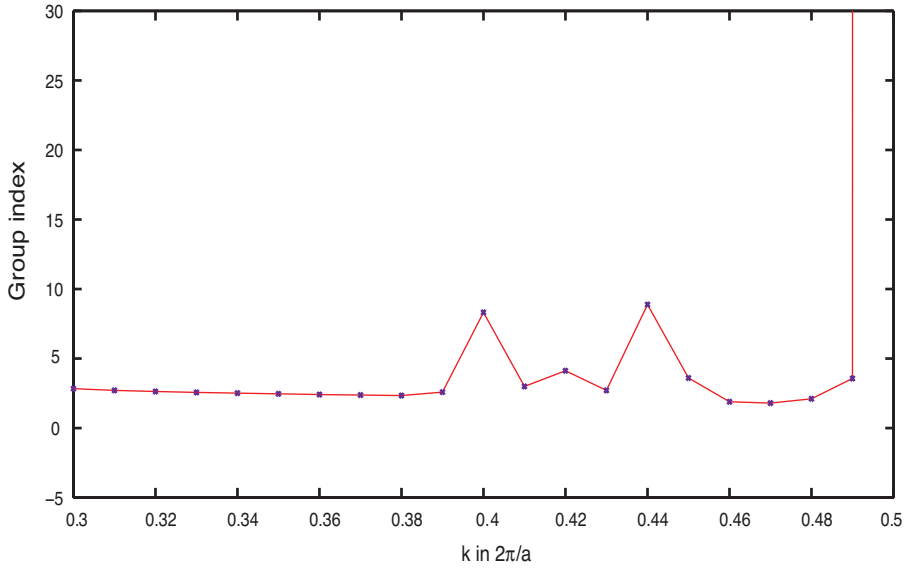

Figure 3. 11.- Group index n_g as a function of the wavenumber k in the first Brillouin zone for the corrugated waveguide.

In this case two relatively high values of the group index $\left(n_g = 8\right)$ are achieved for $k = 0.4$ and $k = 0.44$. For $k > 0.49$ the group index grows abruptly which in turns enhance the slow light phenomenon.

3.3.3.- Transmission and reflection spectra.

We carried out an analysis on the transmission and reflection spectra for the device using the FDTD simulations software. We modeled this device in 3D. The spectra are shown in the Figure 3. 12 for this case.

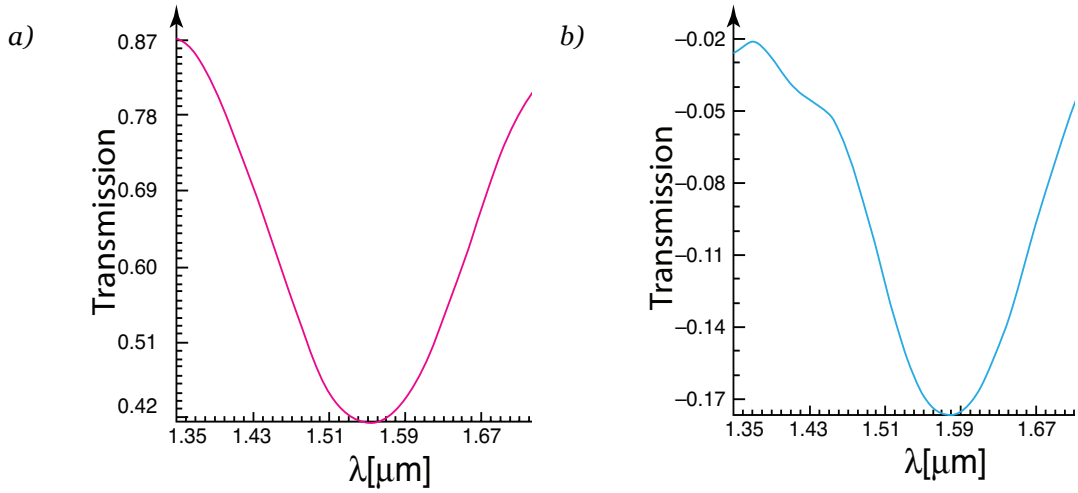

Figure 3. 12.- a) Transmission and b) reflection spectra for the corrugated shown in the Figure 3. 8.

The reflection and transmission spectra are normalized to one. We can observe 42% of transmission and 17% of reflection around $\lambda = 1550$ nm. The rest of the light (41%) can be related with scattering in the y and z direction.

Note that we can get values of group index relatively high for this particular wavelength; however our simulations show that at shorter wavelengths the transmission increases and the index groups grow dramatically, see Figure 3. 10.

3.3.4.- Loss analysis.

We also carried out loss analysis similar to strip waveguide and the results are plotted in the Figure 3. 13.

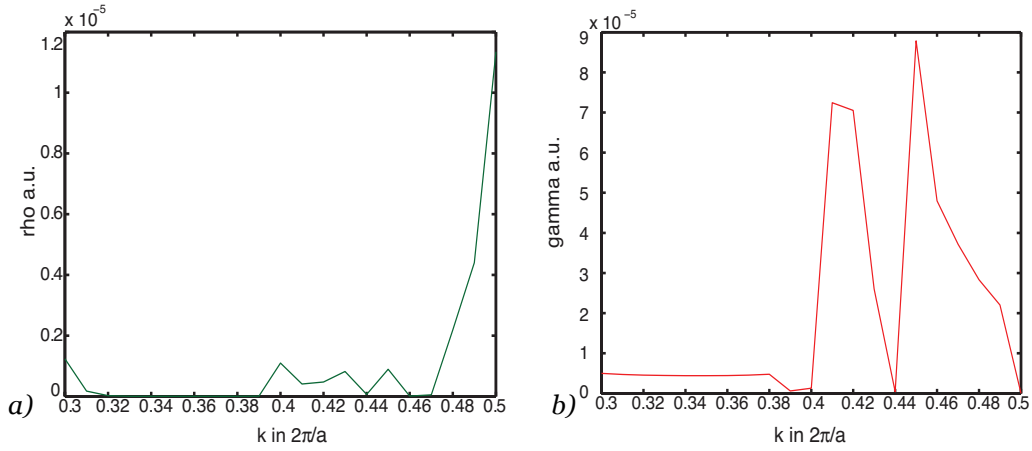

Figure 3. 13.- (a) Backscattering vs k, and (b) Out of plane scattering vs k for corrugated photonic crystal waveguide.

We observe that backscattering loss has low values in the Brillouin zone. Although near to its border, for $k = 0.5$, the backscattering increases up to $1.16X10^{-5}$ dB/cm, see Figure 3. 13 (a).

In the out of plane radiation losses case, these losses are relatively high compared with backscattering losses, especially for $k > 0.4$ along the first Brillouin zone.

To obtain the total losses we substituted the previous values of the last coefficients ρ and γ in the equation (2.25),and this is shown in the Figure 3. 14.

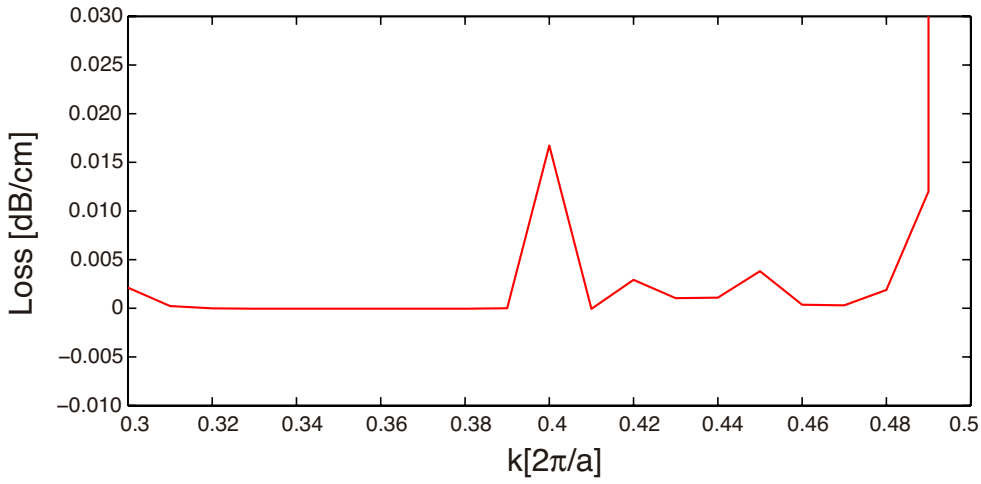

Figure 3. 14.- Total losses variations in the first Brillouin zone for the corrugated waveguide.

Here we can observe that the higher losses are for $k > 0.48$. Note that the same region of the Brillouin zone, the values of the group index are the highest as it is shown in the Figure 3. 11. Also we can note an almost lineal scaling of the total losses respect to group index.

For comparison purposes we can note that for values of $k = 0.4$ we can get group indexes $n_g \approx 10$ (Figure 3. 11) without significant losses (0.015 dB/cm) as it shown in the Figure 3. 14.

Note that the total loss for this structure is two orders of magnitude lower than that of strip waveguide.

3.4.- References

- Ampere A. Tseng, *et al.,* Electron Beam Lithography in Nanoscale Fabrication: Recent Development. *IEEE Transactionson electronics packingmanufacturing* ***26***, (2003).
- Jaime García, *et al.,* 1D periodic structures for slow-wave induced non-linearity enhancement. *Optics Express* ***16*** (5), 3146, (2008).
- L. O'Faolain, *et al.,* Loss engineered slow light waveguides. *Optics Express* ***18*** (26), (2010).
- M. Notomi, *et al.,* Systematic design of flat band slow light in photonic crystal waveguides. *Optic Express* ***15*** (26), (2007).
- M. Rothschild, *et al.,* Nanopatterning with UV Optical Lithography. *Mrs Bulletin* ***30***, (2005).
- OFaolain, *et al.,* Loss engineered slow light waveguides. *Optics Express* ***18*** (26), 27627, (2010).
- S. G. Johnson, *et al.,* Block-iterative frequency-domain methods for Maxwell's equations in a planewave basis. *Optics Express* ***8*** (3), 173–190, (2001).
- solutions, F. (n.d.). *FDTD Solutions*. Retrieved from FDTD Solutions: http://www.lumerical.com/tcad-products/fdtd/

Chapter 4.- Conclusions.

4.1.- Conclusions.

We theoretically and numerically studied two slow-light structures based on 2-D periodic crystal waveguides: the strip waveguide with holes and a corrugated waveguide. We choose these structures because of their relative fabrication simplicity compared to other waveguides already reported in the literature.

Our studies and simulations included the design and optimization of the size of the structures for obtaining a large constant group index in a high bandwidth, as well as for obtaining minimum propagation loss through the waveguides. We used two numerical methods for the design and modeling of these devices: Plane Wave Expansion (PWE) and Differences Finite in Time Domain (FDTD).

From our simulations, we found that the strip waveguide with silica holes shows slow light properties with n_g about 8.5 at a bandwidth of 14 nm. For the second band, the dispersion curve show a relatively flat and monomode behavior near λ = 1550 nm. In this structure we observe a relatively low extrinsic losses (1.3 dB/cm) around $k = 0.42$ where we can get values of group index close to $n_g \approx 15$. In this structure, the extrinsic losses caused by the backscattering and out of plane scattering are not significant enough to become a sensible limitation for producing this promising slow light waveguide structure.

For the corrugated waveguide, we obtained values of $n_g \approx 7.8$ at the edge of the third band, where it is flat and monomode around λ = 1550 nm. We found that at short wavelengths (compared to 1550 nm) high transmission of the light can be obtained with values as large as 23 for the index group. We also notice that for values of $k = 0.4$, the group index of the structure is $n_g \approx 10$

without significant losses (0.015 dB/cm). Specific features of this proposed structure makes quite a promising device, such as: a high efficiency coupling, access to the waveguide, high bandwidth and field confinement at slow light.

One promising application for our proposed slow light devices is the development of a slow-light spectrometer on chip, more specifically an arrayed waveguide gratings (AWG) spectrometer. The spectral resolution of such spectrometers is enhanced when the group index grows.

In this thesis we analyzed the extrinsic losses in the slow-light regimen, we leave pending the mode coupling efficiency using adiabatic transitions. Preliminary studies show that the introduction of adiabatic transitions improves the mode coupling in the device thereby enhancing the transmission along the structure.